NASA TECHNICAL NOTE

NASA TN D-3490

NASA TN D-3490

LONGITUDINAL AND LATERAL-DIRECTIONAL AERODYNAMIC CHARACTERISTICS OF A LARGE-SCALE, V/STOL MODEL WITH FOUR TILTING DUCTED FANS ARRANGED IN A DUAL TANDEM CONFIGURATION

by Demo J. Giulianetti, James C. Biggers, and Ralph L. Maki

Ames Research Center
Moffett Field, Calif.

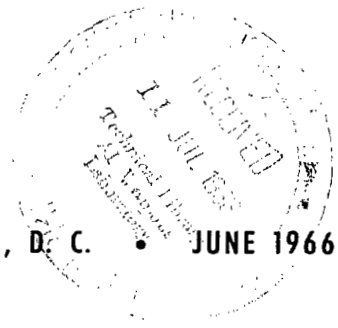

NATIONAL AERONAUTICS AND SPACE ADMINISTRATION • WASHINGTON, D. C. • JUNE 1966

LONGITUDINAL AND LATERAL-DIRECTIONAL AERODYNAMIC CHARACTERISTICS OF A LARGE-SCALE, V/STOL MODEL WITH FOUR TILTING DUCTED FANS ARRANGED IN A DUAL TANDEM CONFIGURATION

By Demo J. Giulianetti, James C. Biggers, and Ralph L. Maki

Ames Research Center
Moffett Field, Calif.

NATIONAL AERONAUTICS AND SPACE ADMINISTRATION

For sale by the Clearinghouse for Federal Scientific and Technical Information
Springfield, Virginia 22151 – Price $3.00

LONGITUDINAL AND LATERAL-DIRECTIONAL AERODYNAMIC CHARACTERISTICS OF A LARGE-SCALE, V/STOL MODEL WITH FOUR TILTING DUCTED FANS ARRANGED IN A DUAL TANDEM CONFIGURATION

By Demo J. Giulianetti, James C. Biggers, and Ralph L. Maki
Ames Research Center

SUMMARY

Differential fore-aft duct exit vane deflection and differential fore-aft thrust were effective for pitching-moment trim at the low and high duct incidences, respectively. Proper phasing of these controls would be necessary for longitudinal trim in the intermediate duct incidence range from 40° to 70° where the trim requirements reached a maximum. Thrust vectoring by the use of differential fore-aft duct incidence was effective in reducing these trim requirements.

INTRODUCTION

There has been much recent interest in the use of tandem arrangements of tilting ducted fans as both propulsive units and lifting devices for vertical and short takeoff and landing (V/STOL) aircraft. Such a ducted fan arrangement would provide an aircraft with powerful longitudinal and lateral-directional control, especially at low-speed and hovering flight conditions. Other advantages of ducted fans are their compactness, compared to the size of free propellers and rotors required for the same thrust, and the contribution of shroud lift to total lift at forward speed. However, a tandem ducted fan arrangement can cause several problems such as duct stall, trim changes with changes in duct incidence at transition forward speeds, aerodynamic interference due to fore-aft duct placement and lateral-directional cross-coupling effects at sideslip with the ducts at high incidence angles.

Early small-scale studies of this concept have been reported in reference 1 where the effects of duct placement, an aft wing, and wing tips were investigated. In a later investigation of a small-scale model with dual tandem ducted fans (ref. 2), using duct exit vanes as a primary yaw control in hover caused cross-coupling effects that resulted in adverse rolling moments. It was also shown that stall on the upper outside duct surfaces in transition contributed to poor lateral-directional behavior of the model, especially in the approach speed range. However, it was noted that the duct stall characteristics could be subject to scale effects. A need for investigating basic aerodynamic characteristics and performance parameters of full-scale ducted fans was pointed out in references 3 and 4 and no known additional full-scale information has since been obtained; hence such information is still scarce.

The present investigation was therefore made of a large-scale, complete model of a typical V/STOL aircraft having four tilting ducted fans arranged in tandem pairs. General longitudinal and lateral-directional aerodynamic characteristics were determined. Performance, stability, control, and the effects of duct stall were investigated through a speed range from hovering to cruising flight. The effects of fuselage angle of attack, differential fore-aft duct incidence and fan speed settings, differential fore-aft and left-right duct exit vane deflection, and sideslip were determined. Vertical-tail effectiveness was briefly investigated.

Tests were conducted at forward speeds ranging from 0 to about 94 knots. Duct incidences tested ranged from 80° on the four ducts (near hover configuration) to 5° on the front and 0° on the rear ducts (cruise configuration).

NOTATION

b	span of wing, ft
c	reference length, wing chord, ft
$\bar{c}$	vertical-tail mean aerodynamic chord, in.
C_D	drag coefficient, $\frac{D}{qS}$
C_L	lift coefficient, $\frac{L}{qS}$
C_l	rolling-moment coefficient, $\frac{\text{rolling moment}}{qSb}$
C_m	pitching-moment coefficient, $\frac{M}{qSc}$
C_n	yawing-moment coefficient, $\frac{\text{yawing moment}}{qSb}$
C_Y	side-force coefficient, $\frac{\text{side force}}{qS}$
d	fan diameter, ft
D	drag, lb
i	incidence, deg
J	fan advance ratio, $\frac{V}{nd}$
L	lift, lb
M	pitching moment, ft-lb

mc	moment center
N	fan rotational speed, rpm
n	fan rotational speed adjusted to standard sea level temperature, $\frac{N}{60\sqrt{\theta}}$, rps
P_o	standard atmospheric pressure, 2116 lb/sq ft
P_s	test-section static pressure, lb/sq ft
q	free-stream dynamic pressure, lb/sq ft
S	reference area, area of wing, sq ft
T	thrust along fan axis, lb
T_c	thrust coefficient, $\frac{T}{qS}$
T_s	maximum measured reference static thrust of the model, 5400 lb
V	free-stream velocity adjusted to sea-level, standard conditions, fps or knots
Y	side force, lb
α	fuselage angle of attack, deg
β	sideslip angle, deg
Δ	increment from average value
δ	relative static pressure, $\frac{P_s}{P_o}$
δ_D	duct incidence relative to fuselage, deg
δ_e	fore-aft duct exit vane deflection relative to fan thrust axis, deg
δ_a	left-right duct exit vane deflection relative to fan thrust axis, deg
θ	relative temperature ratio, ambient temperature (absolute)/460° F

Subscripts

a	aft
f	forward

l	left
r	right
t	wing tips
u	untrimmed
1,2	moment centers 5 percent of the distance between the duct rotation points, respectively, ahead of and behind the model moment center located midway between the duct rotation points.

Examples of Duct Incidence and Exit Vane Deflection Notation

$\delta_D = 40^\circ$	all four ducts at 40° incidence
$\delta_{D_f}/\delta_{D_a} = 35^\circ/45^\circ$	$\pm 5^\circ$ fore-aft differential duct incidence; forward ducts at 35° and aft ducts at 45°
$\delta_{e_f}/\delta_{e_a} = -20^\circ/20^\circ$	$\pm 20^\circ$ fore-aft differential duct exit vane deflection (total of 40° deflection); positive total deflection when vane trailing edges are up on the forward vanes and down on the rear vanes
$\delta_{a_l}/\delta_{a_r} = 20^\circ/-20^\circ$	$\pm 20^\circ$ left-right differential duct exit vane deflection (total of 40° deflection); positive total deflection when vane trailing edges are down on the left vanes and up on the right vanes

MODEL DESCRIPTION

Photographs of the model installed in the test section of the Ames 40- by 80-foot wind tunnel are shown in figure 1. Model geometry and dimensional data are given in figure 2. Additional pertinent dimensional data of the model are given in table I.

Wing Geometry

Front fairings.- The model had short span fairings between the fuselage and the front ducts that housed the front duct drive shafts and trunnion tubes. These fairings had NACA 64A420 sections that were modified by removal of the aft lower surface concavity with a straight line from the trailing edge tangent to the lower surface.

Wing.- The wing incidence was 3° with respect to the fuselage. Aspect ratio was 2.5 based on wing area with allowances for cutouts to accommodate the rear duct attachments and rotation. The rear duct rotation point was 1.1 inches above the wing chord at that station. Rear duct drive shafts and

trunnion tubes were contained in the wing. The airfoil was an NACA 64A420 section modified by increasing the chord 19 percent at the trailing edge. The modified upper and lower surfaces were straight lines from the original 60 percent chord to the extended trailing edge.

Wing tips.- Variable incidence wing tips having NACA 64A415 sections were located outboard of the rear ducts. Incidence was measured with respect to the fan thrust axis and was 0° for this investigation except for brief studies with the wing tips removed and at -10° incidence.

Ducted Fans

The ducted fans used in this investigation are described in reference 3 and are the same type as those used in references 3 and 4, except that the blade angle was increased to 23° at the tip and the inlet guide vanes were undeflected. For convenience, the shroud and centerbody coordinates from reference 3 are listed in table II.

Duct exit vanes.- The duct exit vanes are described in table I and figure 2(a). They were capable of $\pm 20^\circ$ of deflection about the fan thrust axis. The vanes were mounted with their leading edges extending into the duct exit and were pivoted at the quarter chord line which was located 0.75 inch behind the duct trailing edge.

Fan drive system.- Each pair of front and rear ducted fans was independently powered by a 1000 horsepower electric motor mounted in the fuselage. Motor power was transmitted through central tee gear boxes and appropriate shafting to transmissions in the fan centerbodies that rotated with the ducts. Input power to the motors was measured on wattmeters.

Simulated Engine Nacelles

Simulated turbojet-engine nacelles were mounted on the wing between the fuselage and the rear ducts. The nacelles were ducted for through-cold flow which exited at the bottom rear of each nacelle. Details of the nacelles are given in figure 2(b).

TESTS AND PROCEDURE

Longitudinal and lateral-directional aerodynamic characteristics were obtained for various duct incidences at forward speeds ranging from 0 to about 94 knots. Forward speeds were chosen to represent approximately zero drag at 0° angle of attack, as well as climb and descent conditions, for a fixed duct incidence and fan speed. The general method of testing was to vary fuselage attitude while duct incidence, fan speed, and forward speed remained fixed. Angle of attack was varied from -8° to 22° at sideslip angles from 0° to 12°. The method and procedure for obtaining isolated ducted fan data were the same as those of reference 2.

Differential fore-aft thrust was obtained by varying front duct fan speed with the rear duct fan speed constant. Thrust vectoring was obtained by differential fore-aft settings of duct incidence and exit vane deflection. Duct incidences tested ranged from 20° to 80° on all four ducts for equal duct incidence settings and from 5° to 65° on the front ducts and 0° to 75° on the rear ducts with 5° and 10° differential duct incidences. Duct incidence was not carried to 90° because of problems with recirculating duct exit flow. Total differential fore-aft and left-right duct exit vane deflections tested ranged from 0° to 40°. Fan speeds were varied from about 1100 to about 3600 rpm with the majority of testing done at about 2200 rpm. Limited data were obtained with the wing tips and vertical tail removed.

Duct stall was investigated at duct incidences of 40°, 45°, 50°, and 60° and was indicated by fluctuations in front duct fan speed with no change in power input. The procedure for stalling the ducts was to simultaneously decrease front and rear duct fan speeds in equal increments until the ducts stalled and then to gradually increase the front and rear duct fan speeds to reattach the flow. No attempt was made to investigate duct stall at duct incidences greater than 60° because of the low relative crossflow velocities involved.

CORRECTIONS

No corrections were applied to the force and moment data to compensate for wind-tunnel wall interference effects as the magnitude of such corrections was not known. A drag correction of 3.4 lb/lb/sq ft of dynamic pressure was estimated and applied to the drag and pitching-moment data to compensate for free-stream effects on the exposed horizontal model support tube and the exposed strut tips. This drag correction did not account for any effects of the front duct slipstream impinging on the horizontal model support tube as the front duct incidence was changed.

RESULTS

The static thrust of the model and that of four isolated ducted fans are compared in figure 3. Isolated ducted fan thrust coefficient as a function of advance ratio is shown on figure 4. Longitudinal aerodynamic characteristics of the model are presented in figures 5 through 11. Lateral-directional aerodynamic characteristics of the model are presented in figures 12 through 15. The results of figures 8(d), 14(b), and 15(e) were made dimensionless by dividing the absolute forces and moments by the maximum measured model static thrust of 5400 pounds (fig. 3). Estimated performance of a 6500 pound gross weight airplane having the same configuration as the model investigated is shown in figures 16 through 22. These figures are indexed in table III for convenient reference.

DISCUSSION

Thrust

The static thrust of the model and four times that of an isolated ducted fan of the same type as those installed on the model is shown in figure 3. The results show little or no static thrust difference between the model and the isolated ducted fans, indicating negligible interference effects at zero forward speed. To aid in the interpretation and usability of the test results, isolated ducted fan thrust coefficient, T_c, is shown as a function of advance ratio in figure 4. The isolated ducted fan thrust was obtained from measurements with strain gages located on the ducted fan trunnion tube mount.

Longitudinal Aerodynamic Characteristics

Lift.- Lift coefficient generally increased with angle of attack to high angles of attack for configurations with equal and differential fore-aft duct incidences (figs. 5 and 6). There were no large, sudden losses of lift or increases in drag (duct incidence fixed), indicating no abrupt duct or wing stall. However, variations of pitching-moment coefficient for these data indicated some degree of flow disturbance at the higher duct incidences at moderate angles of attack.

Longitudinal stability.- The pitching-moment results of figures 5 and 6 indicate some variations in static stability that often occurred within a small angle-of-attack range. For duct configurations with pitching-moment curves that remained linear through portions of an angle-of-attack range, the stability was either nearly neutral, such as at the cruise and near cruise duct incidences (figs. 5(a), (b) and 6(a), (b)), or unstable at the higher duct incidences. The static stability for this model at cruise conditions was less than what would have been expected for a moment center midway between pairs of fore and aft ducted fans. A fore-aft shift of this moment center of 5 percent of the distance between duct rotation points (mc_1 and mc_2, respectively) resulted in a change in static stability at the low duct incidence, cruise configuration (fig. 7). This effect decreased with increased duct incidence. This is to be expected since, at cruise conditions, pitching moment is largely the result of aerodynamic forces produced by the wing, and changing the moment center changes C_{m_α}. However, at the low forward speeds associated with high duct incidences, the wing forces are small or negligible and pitching moment changes are largely the direct result of changing the moment arms to the front and rear ducted fan thrust lines.

Longitudinal stability at low duct incidences is further affected by the countereffects of the slipstream dynamic pressure and downwash from the front ducted fans which respectively increase and decrease C_{L_α} of the wing and rear ducts.

Longitudinal control.- Longitudinal control for maneuvering and trim can be accomplished by the use of differentially deflected fore-aft duct exit

vanes at low duct incidences (cruise conditions) and by differential fore-aft thrust or thrust vectoring at high duct incidences (low forward speed conditions).

Longitudinal trim requirements at equal and differential fore-aft duct incidences generally increased with increases in duct incidence (figs. 5 and 6). The effectiveness, in terms of ΔC_m, of $\pm 20^\circ$ of differential fore-aft duct exit vane deflection at $\alpha = 0^\circ$ remained relatively constant to about 60° of duct incidence. As a result, the duct exit vanes became inadequate as trim devices beyond about 40° of duct incidence although pitch control effectiveness was maintained over a sizable angle-of-attack range to about 60° duct incidence. Hence, to maintain longitudinal control throughout the transition duct incidence range, differential fore-aft thrust could be phased in at the intermediate duct incidence range of 40° to 60°. Differential fore-aft thrust was obtained for these tests by varying front duct fan speed with the rear duct fan speed constant. The model characteristics for these conditions are shown in figure 8. Variable fan speed rather than blade angle changes was used to vary thrust because of the greater difficulty involved in blade angle changes.

The variable incidence wing tips outboard of the rear ducts were intended to function as horizontal stabilizers in cruising flight. The wing tips had little effect on the model characteristics at the cruise duct configuration (fig. 9(a)), but resulted in reduced pitching-moment coefficients over a large angle-of-attack range at 50° duct incidence for a wing tip incidence of 0° (fig. 9(b)). Changing the wing tip incidence to -10° had little effect on pitching-moment coefficient both at the cruise duct configuration and at 50° of duct incidence.

Duct stall.- Duct stall was measured at duct incidences from 40° to 60°. Incipient duct stall was intermittent and was recognized by fluctuations in fan speed with no change in input power (fig. 10). It was not severe and had little effect on the model aerodynamic characteristics (fig. 11); thus it was a conservative indication of duct stall. A more meaningful measure of duct stall in terms of a stall boundary for flight would be based on factors found in duct stalls more severe than encountered in these tests. They would result in high vibration, high blade stresses, and significant changes in aerodynamic characteristics. Duct stall occurred only on the front ducts suggesting that the downwash of the front ducts on the rear ducts delayed rear duct stall. Outer surface duct stall as noted in reference 2 was not encountered in this investigation. Descent conditions as affected by duct stall are discussed with performance.

Lateral-Directional Aerodynamic Characteristics

Directional stability.- Directional stability was determined from the model lateral-directional aerodynamic characteristics at sideslip presented in figure 12. The vertical-tail volume was sufficient for directional stability to high sideslip angles for the cruise duct configuration; however, the model was directionally unstable at low sideslip angles at 30° and 50° duct incidence (fig. 13). Similar effects are discussed in reference 2 where it was

shown that increasing the vertical tail area made little difference in model directional stability until transition flight speeds, corresponding to 30° duct incidence or less, were reached.

Lateral-directional control.- Lateral-directional control throughout a transition duct angle range would require the use of both differential left-right duct exit vane deflection and differential left-right blade angle changes. Adverse roll and yaw cross-coupling effects occurred when differentially deflected vanes were used as a roll control at low duct incidence (cruise conditions) and as a yaw control at high duct incidence (hover conditions) (fig. 14). The roll and yaw control with ±20° of differential left-right duct exit vane deflection at cruise and 80° duct incidences, respectively, was maintained over a large angle-of-attack range at 0° and 8° of sideslip (figs. 15(a), 15(b), and 15(e)). The roll control at the cruise duct configuration was accompanied by yaw cross coupling that was favorable at negative angles of attack but became adverse at positive angles of attack (figs. 15(a) and 15(b)). As expected, large adverse roll-yaw cross coupling occurred at the intermediate duct incidence of 50° (figs. 15(c) and 15(d)). Although not tested, differential left-right thrust as a roll control at high duct incidences would be accompanied by favorable yaw cross coupling. Thus the need for careful phasing of these controls for properly separating roll and yaw at the midtransition speeds becomes apparent. High values of C_{l_β} at high angles of attack accompanied by adverse yaw as shown in figure 12 indicate the tendency for Dutch roll oscillations reported in reference 2. It should be noted that sideslip greatly changed the roll control effectiveness of the exit vanes with changes in angle of attack at 50° duct incidence (figs. 15(c) and 15(d)).

Transition Performance

General transition characteristics.- The test results were used to derive a transition from hover to cruising flight for an airplane having tilting, dual tandem, ducted fans. Such a transition would be accomplished by a programmed series of changes in duct incidence and power with changes in forward speed. The required variation of duct incidence with forward speed from hover to cruise flight for a 6500 pound gross weight airplane having this configuration is shown in figure 16 for 0° angle of attack and pitching moments trimmed. The power required for this transition is shown in figure 17. The differences in forward speed resulting from pitching-moment trim were small and were negligible for a ±5° differential duct incidence compared to those for equal duct incidence settings. Only results for differential duct incidence settings were available where such settings are noted in figure 16 at the higher forward speeds.

Pitching-moment variation with duct incidence.- The untrimmed pitching moments for zero control deflection increased with increases in duct incidence and reached a maximum at about 60° duct incidence (approximately 45 knots forward speed) (fig. 18). Fore-aft differential duct incidence settings of ±5° resulted in reduced pitching-moment trim requirements. A forward shift of the moment center of 5 percent of the distance between duct rotation points (mc_1)

was even more effective in reducing trim requirements than the differential duct incidence settings in the duct incidence range of maximum pitching moments.

Control power variation with duct incidence.- A differential duct exit vane setting of ±20° was effective for trim to about 44° of duct incidence (fig. 19). Differential duct incidence settings of ±5° extended the usability of this exit vane deflection for trim to about 50° of duct incidence (approximately an 8 knot reduction in forward speed).

Longitudinal trim through transition was obtained with differential fore-aft duct exit vane deflection from cruise to 40° of duct incidence and with differential fore-aft thrust at duct incidences greater than 50°. A differential vane deflection of 40° (assumed to be a limit for linear response) and differential thrust as limited by front duct stall provided sufficient control for trim and residual control available for maneuvering, especially in the duct incidence range of 60° to 70° where untrimmed pitching moments were largest (fig. 20). A ±5° fore-aft duct incidence differential and a forward shift of the moment center of 5 percent of the distance between the duct rotation points resulted in overall decreased trim requirements and increased the minimum control power available for maneuvering which occurred at about 40° of duct incidence.

Effects of duct stall on performance.- The estimated maximum descent rate of the airplane would be limited by front duct stall to about 600 ft/min at a duct incidence of about 60° (fig. 21). As was noted earlier, a conservative measure of incipient duct stall was obtained, and the duct stall was not severe and had little effect on the model longitudinal aerodynamic characteristics. For these reasons it appeared that the maneuvering ability of the airplane was not seriously restricted by front duct stall. This is further illustrated in figure 22 where estimated front and rear duct fan speed changes, in terms of advance ratio, required for longitudinal trim by differential thrust are shown relative to duct stall boundaries. As is shown in figure 22, model interference effects reduced the duct stall boundary of this configuration over that of the isolated ducts.

CONCLUSIONS

A longitudinal trimmed transition from hover to cruising flight was estimated for a 6500 pound gross weight airplane having tilting, dual tandem ducted fans. Duct incidence and forward speed were varied to provide level, unaccelerated flight conditions through the transition.

Untrimmed pitching moments increased with duct incidence and were a maximum at about 60° of duct incidence. Longitudinal trim through transition was accomplished with differential fore-aft duct exit vane deflection at low duct incidences and with differential fore-aft thrust at high duct incidences. In addition, these controls provided residual control available for maneuvering especially in the duct incidence range of maximum untrimmed pitching moments.

Duct stall did not appear to seriously restrict the descent capabilities of the airplane at high duct incidences. Duct stall was encountered on the front ducts only and indicated that front duct downwash effects on the rear ducts delayed rear duct stall.

The model was directionally stable to high sideslip angles at the cruise duct configuration, but was directionally unstable at low sideslip angles at the higher transition duct incidences.

Ames Research Center
National Aeronautics and Space Administration
Moffett Field, Calif., Mar. 30, 1966

REFERENCES

1. Newsom, William A., Jr.: Aerodynamic Characteristics of Four-Duct Tandem VTOL-Aircraft Configurations. NASA TN D-1481, 1963.

2. Newsom, William A., Jr.; and Freeman, Delma C., Jr.: Flight Investigation of Stability and Control Characteristics of a 0.18-Scale Model of a Four-Duct Tandem V/STOL Transport. NASA TN D-3055, 1965.

3. Yaggy, Paul F.; and Mort, Kenneth W.: A Wind-Tunnel Investigation of a 4-Foot-Diameter Ducted Fan Mounted on the Tip of a Semispan Wing. NASA TN D-776, 1961

4. Mort, Kenneth W.; and Yaggy, Paul F.: Aerodynamic Characteristics of a 4-Foot-Diameter Ducted Fan Mounted on the Tip of a Semispan Wing. NASA TN D-1301, 1962.

TABLE I.- MODEL DIMENSIONAL DATA

Wing	
Area, sq ft	74.30
Chord, ft	5.62
Span, ft	13.63
Aspect ratio	2.5
Taper ratio	1.0
Airfoil section:	
Max. thickness ratio, percent chord	16.8
Position of max. thickness, percent chord	33.6
Wing tips	
Area for one tip, sq ft	5.53
Aspect ratio	0.4
Taper ratio	0.7
Airfoil section	NACA 64A415
Ducts	
Inside diameter, ft	4.00
Outside diameter, ft	4.87
Exit diameter, ft	4.52
Chord, ft	2.75
Diffuser angle, deg	11
Duct exit vanes	
Area for one vane, sq ft	10.3
Aspect ratio	2.0
Taper ratio	0.8
Airfoil section	NACA 0012-64
Fan	
Fan diameter, ft	4.00
Number of blades	8
Blade angle at tip, deg	23
Vertical tail	
Area, sq ft	26.7
Aspect ratio	2.1
Taper ratio	0.4
Tail volume, cu ft	256

TABLE II.- SHROUD AND CENTERBODY COORDINATES

Shroud coordinates tabulated in percent of shroud chord (33.00 in.)		
Chordwise length	Outside radius	Inside radius
0	81.5	81.5
.5	83.4	79.6
.75	83.8	79.0
1.25	84.4	78.4
2.5	85.4	77.2
5.0	86.4	75.8
7.5	87.1	74.9
10.0	87.6	74.2
15.0	88.2	73.3
20.0	88.6	72.9
25.0	↓	72.7
30.0		↓
35.0		
40.0		
45.0		
50.0		
55.0		73.2
60.0		74.1
65.0	88.0	75.1
70.0	87.4	76.1
75.0	86.8	77.1
80.0	85.9	78.1
85.0	85.2	79.1
90.0	84.3	80.1
95.0	83.3	81.1
100.0	82.2	82.0

Centerbody coordinates tabulated in percent of centerbody length (71.5 in.)	
Length	Radius
0	0
.5	2.07
1.25	3.20
2.50	4.46
5.0	6.17
7.5	7.40
10.0	8.31
15.0	9.68
20.0	10.54
25.0	11.01
25.875[1]	11.06
30.0	11.19
32.57[2]	↓
40.0	
50.0	
60.0	
70.0	10.49
72.05[3]	10.14
80.0	7.97
83.20	6.77
90.0	4.03
95.0	2.01
100.0	0

[1]Shroud leading-edge position
[2]Inlet guide vane c/4 line position
[3]Shroud trailing-edge position

TABLE III.- INDEX TO FIGURES

Figure						
1	Model photographs					
2	Model geometry					
3	Static thrust of the four ducted fans					
4	Isolated ducted fan thrust coefficient as a function of advance ratio					
	Longitudinal aerodynamic characteristics					
	Effects of	δ_D, deg	$\delta_{D_f}/\delta_{D_a}$, deg	α, deg	β, deg	$\delta_{e_f}/\delta_{e_a}$, deg
5	Equal fore-aft duct incidence changes	20, 30, 40, 50, 60, 70, 80		var.	0	0, -20/20
6	Differential fore-aft duct incidence changes		5/0, 15/10, 25/35, 35/45, 45/55, 55/65, 65/75	var.	0	0, -20/20
7	Moment center on static stability	30, 60	5/0	var.	0	0
8	Variable front duct thrust	50, 60, 70, 80		0	0	0
9	Wing tips outboard of the rear ducts	50	5/0	var.	0	0, -20/20
10	Duct stall on input power	40, 45, 50, 60		0	0	0, -20/20
11	Duct stall on model characteristics	40, 45, 50, 60		0	0	0, -20/20
	Lateral-directional aerodynamic characteristics					
	Effects of	δ_D, deg	$\delta_{D_f}/\delta_{D_a}$, deg	α, deg	β, deg	$\delta_{a_l}/\delta_{a_r}$ deg
12	Sideslip	30, 50	5/0	var	0, -2, -4, -6, -8, -12	0
13	Sideslip with the vertical tail installed and removed	30, 50	5/0	0, 8	var.	0
14	Differential left-right duct exit vane deflection	80	5/0	0	0	var.
15	Differential left-right duct exit vane deflection at sideslip	50, 80	5/0	var.	0, -8	0, 20/20
	Performance					
16	Duct incidence required for transition from hover to cruise flight; pitching moment trimmed					
17	Power required for transition from hover to cruise flight; pitching moment trimmed					
18	Pitching moment variations with duct incidence changes at unaccelerated flight conditions					
19	Differential fore-aft exit vane deflection required for trim					
20	Longitudinal trim requirements and pitching moment available at unaccelerated flight conditions					
21	Descent velocities as affected by duct stall; pitching moment trimmed					
22	Duct stall margins					

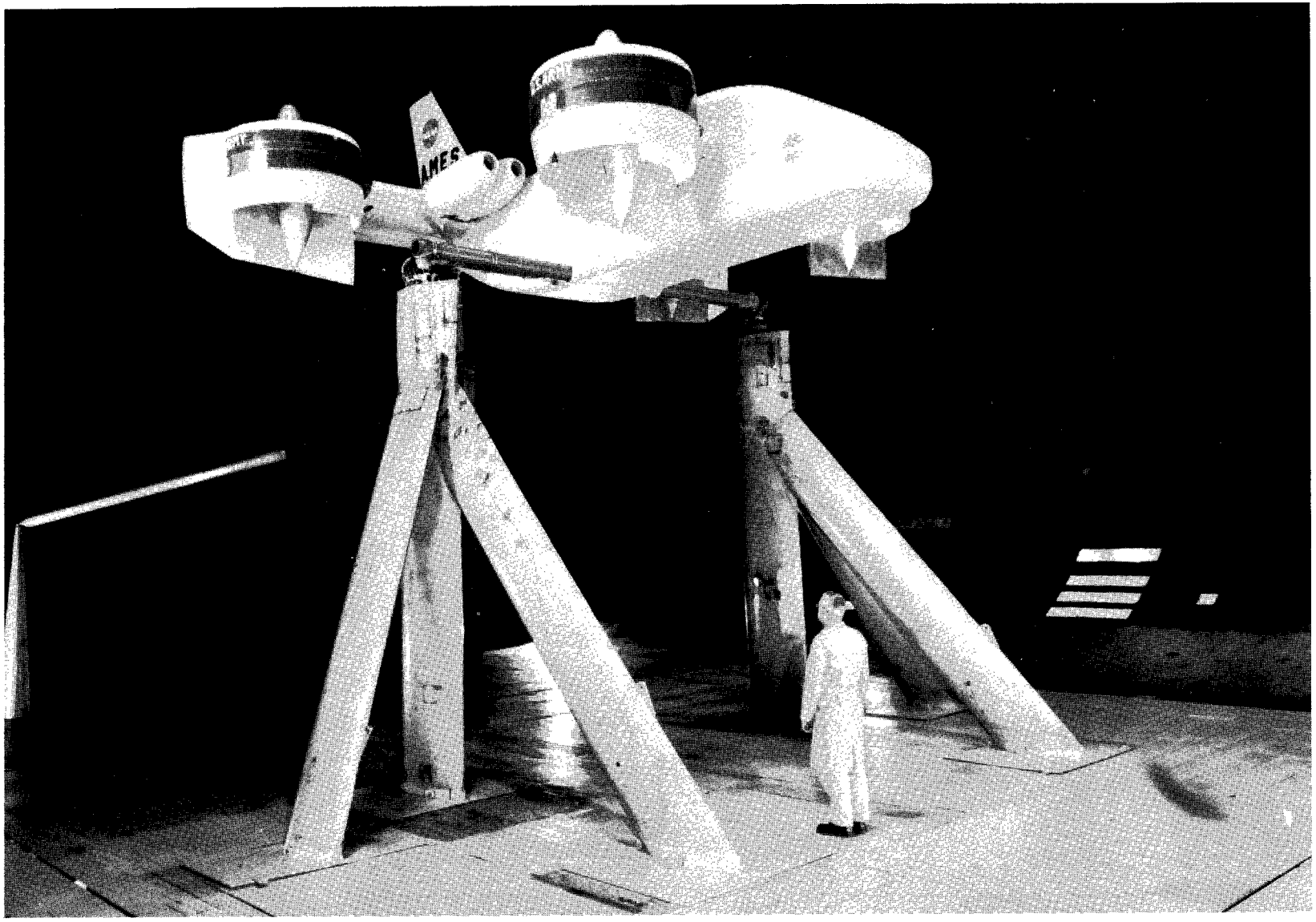

A-33527

(a) Hover duct configuration; $\delta_D = 90^\circ$, $\delta_{e_f}/\delta_{e_a} = 0^\circ/0^\circ$.

Figure 1.- Model mounted in test section of Ames 40- by 80-foot wind tunnel.

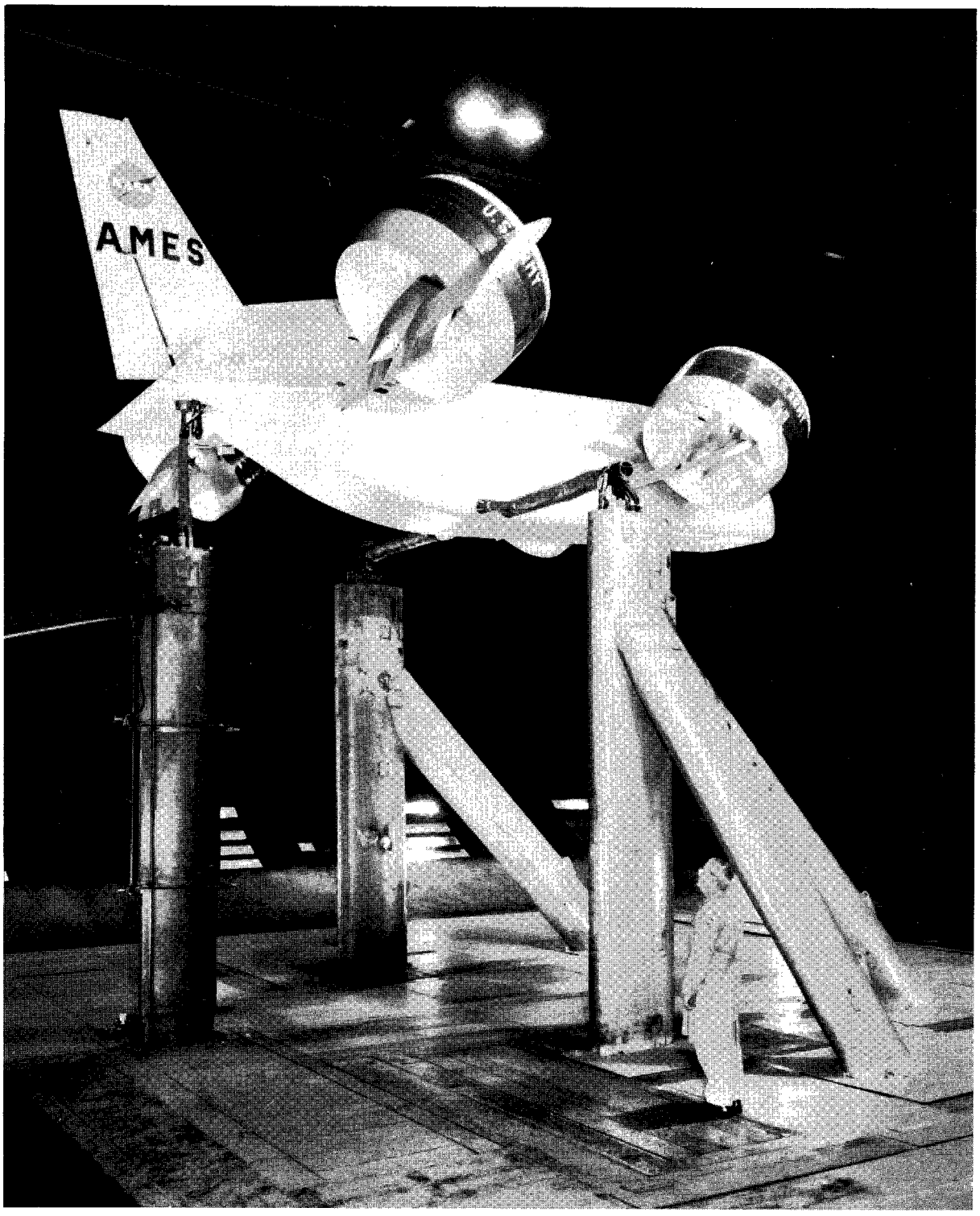

A-33529

(b) Transition duct configuration; $\delta_D = 45^\circ$, $\delta_{e_f}/\delta_{e_a} = -20^\circ/20^\circ$.

Figure 1.- Continued.

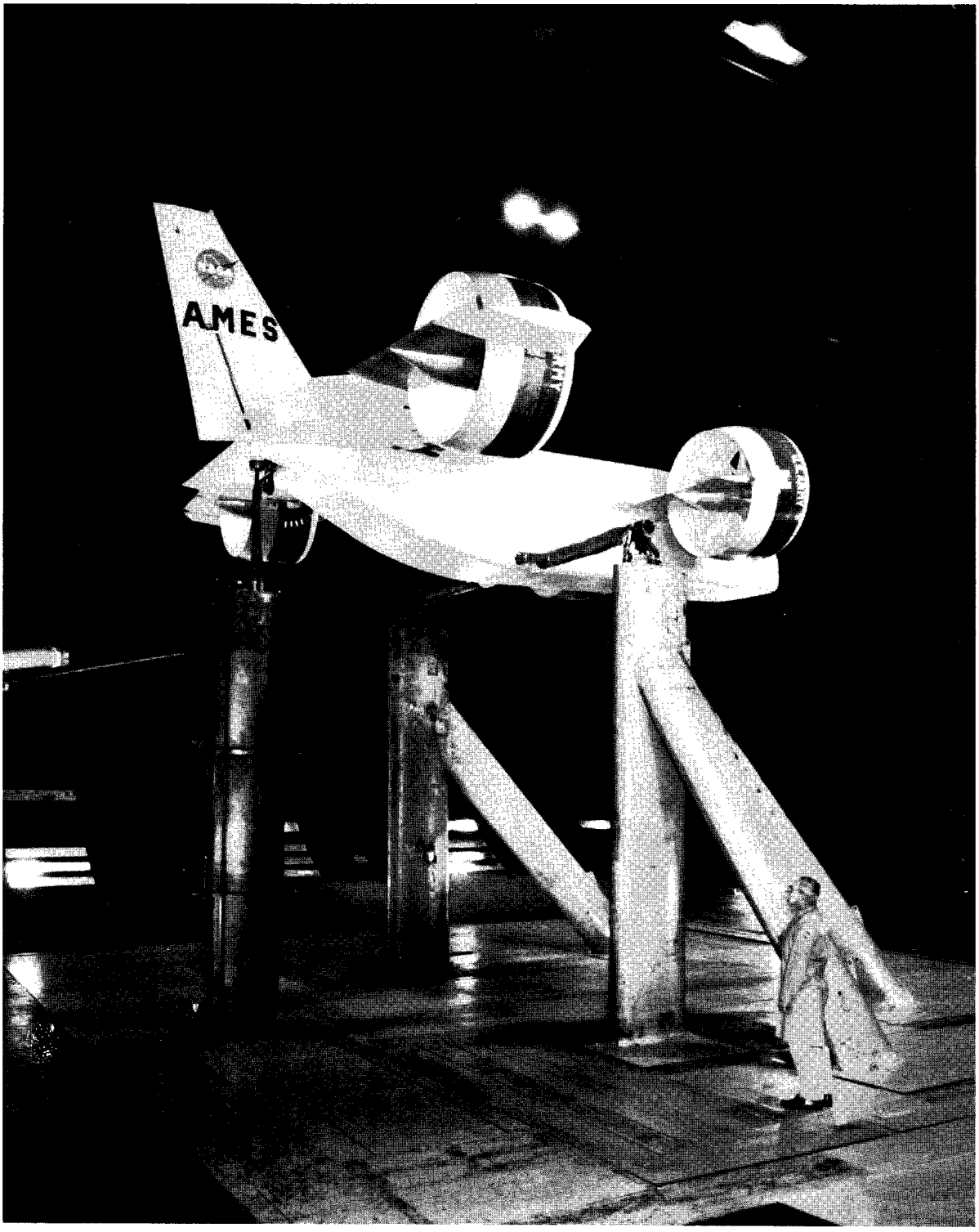

A-33530

(c) Cruise duct configuration; $\delta_{D_f}/\delta_{D_a} = 5^\circ/0^\circ$, $\delta_{e_f}/\delta_{e_a} = 0^\circ/0^\circ$.

Figure 1.- Concluded.

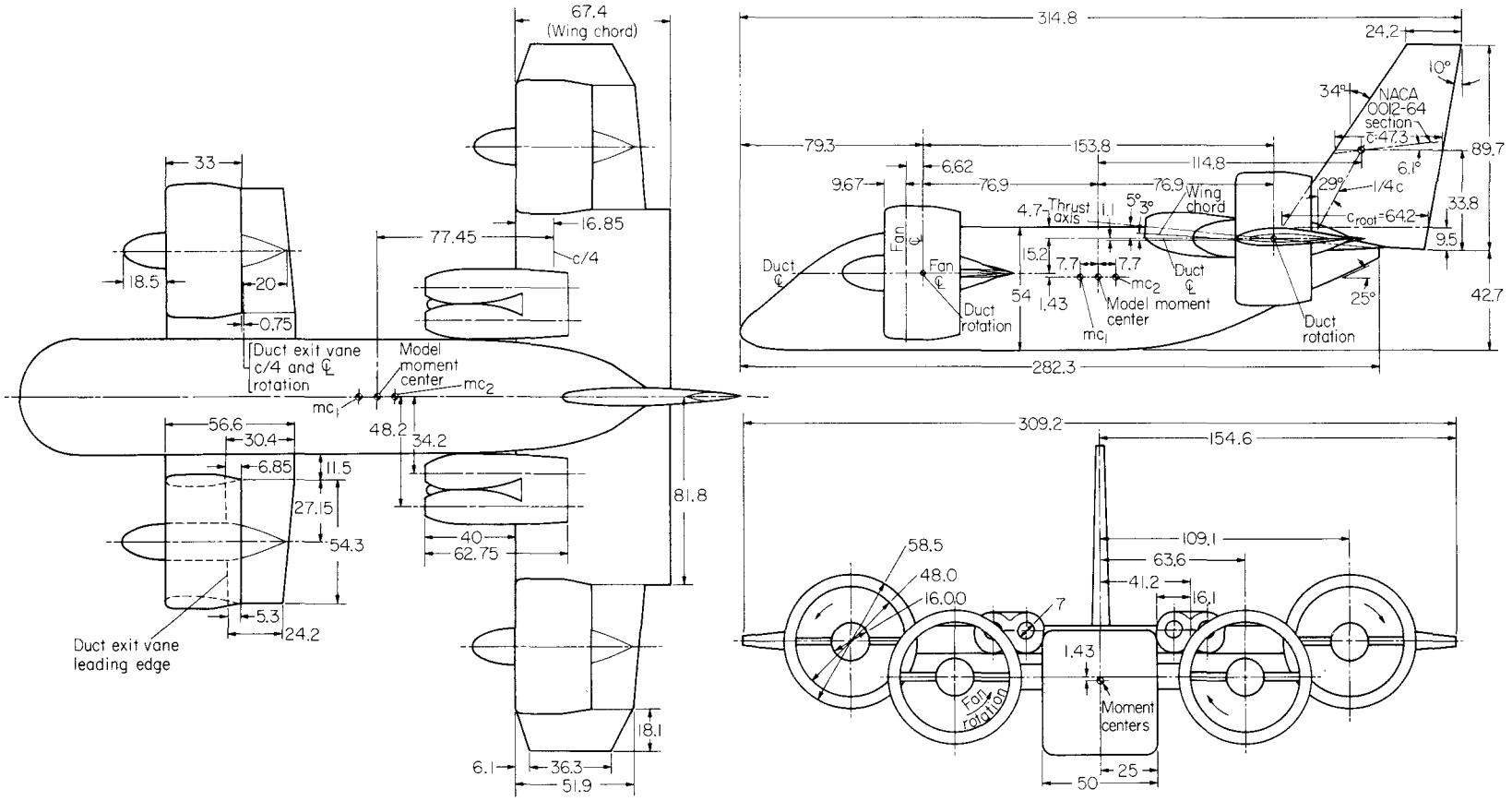

All dimensions in inches

(a) Geometric characteristics of the model.

Figure 2.- Model dimensions and geometry.

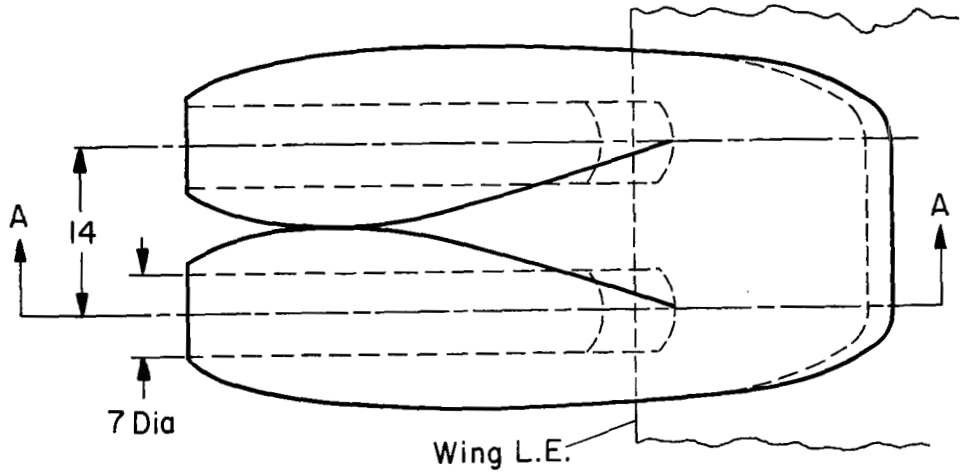

X, inches	R, inches
0	3.69
27.75	8.02
42.75	7.86

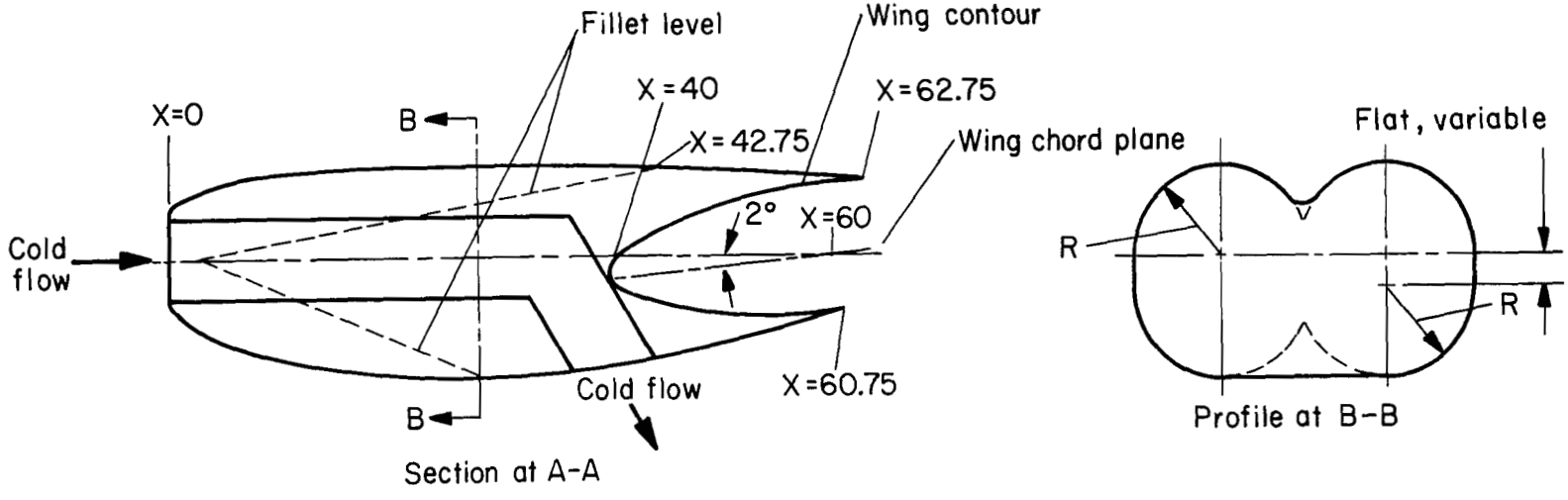

(b) Details of simulated engine nacelles.

Figure 2.- Concluded.

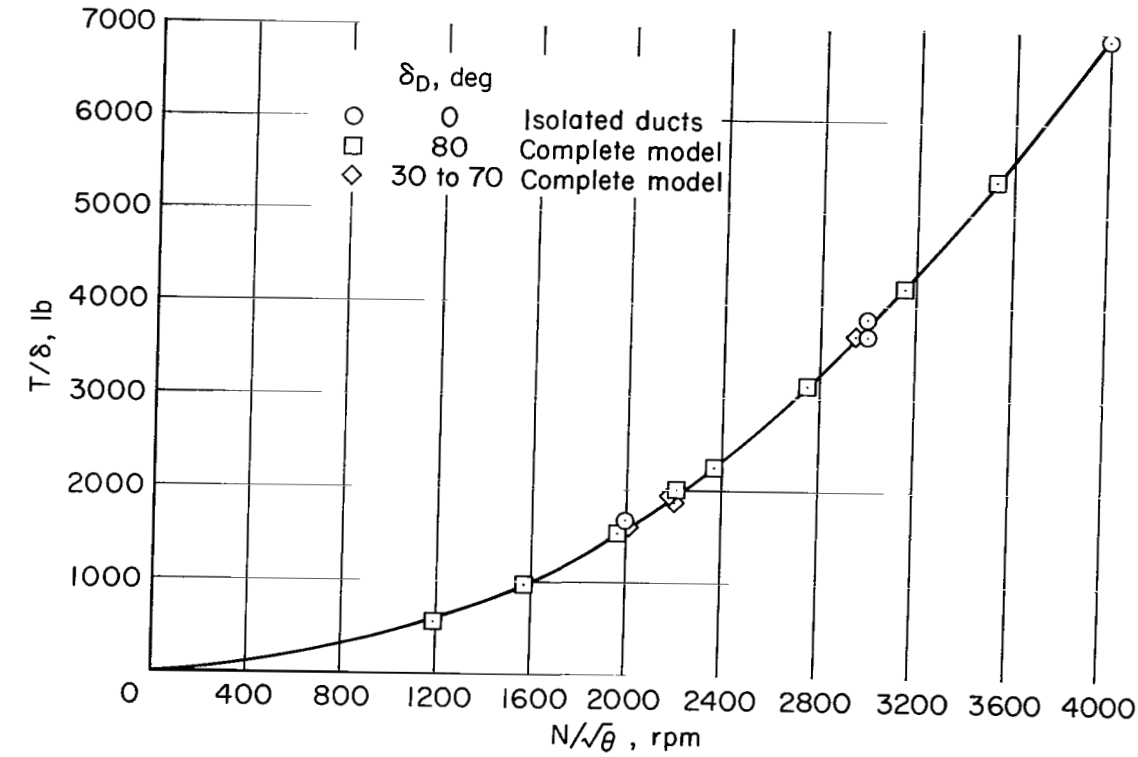

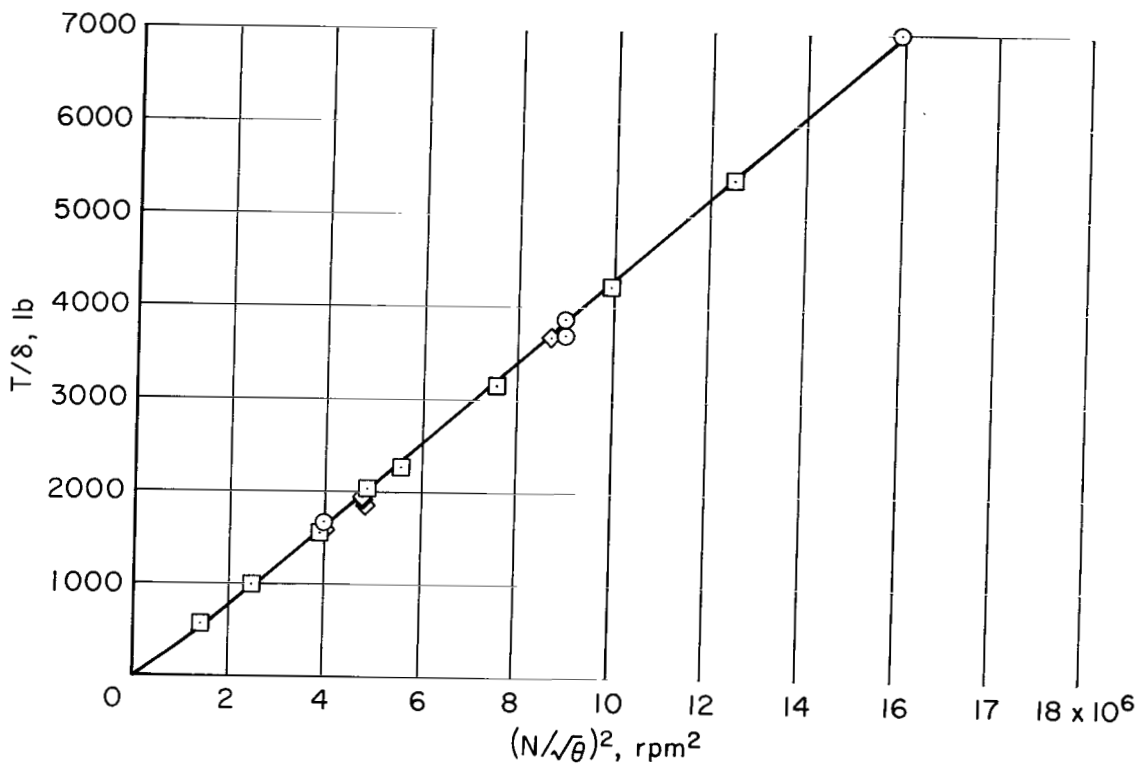

Figure 3.- Thrust at zero forward speed; blade angle = 23°, α = 0°, $\delta_{e_f}/\delta_{e_a}$ = 0°/0°.

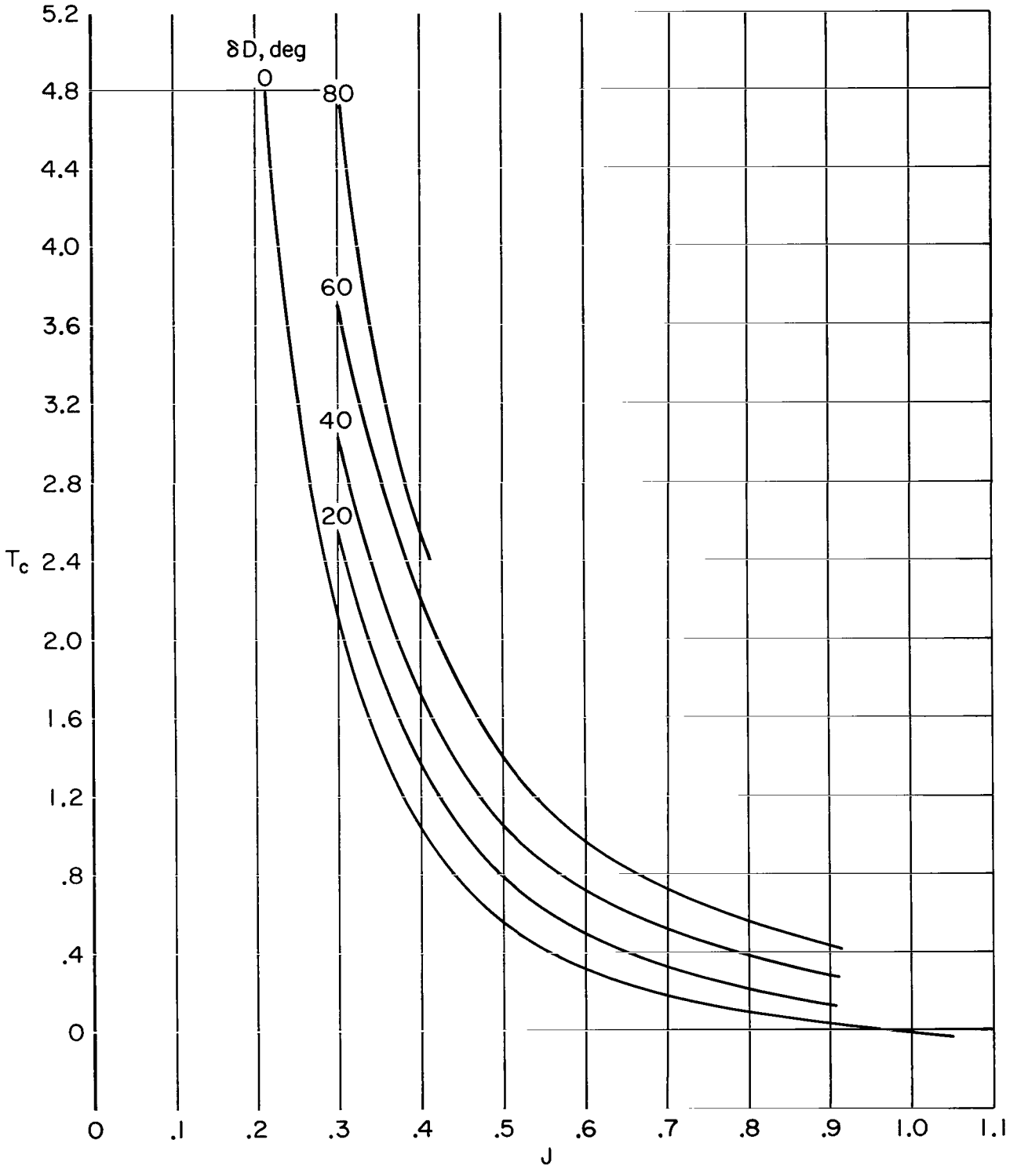

Figure 4.- Thrust coefficient as a function of advance ratio for the isolated ducted fan; blade angle = 23°.

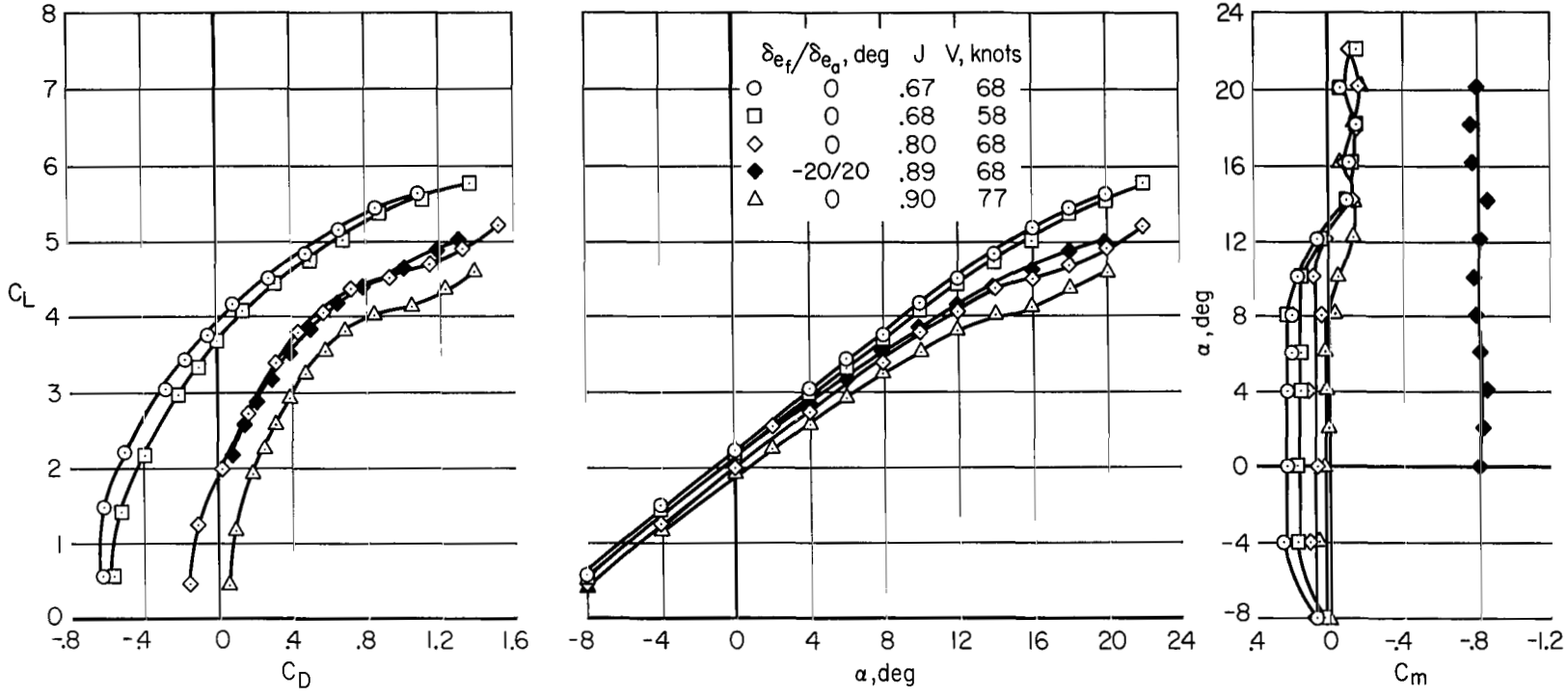

(a) $\delta_D = 20^\circ$

Figure 5.- Longitudinal aerodynamic characteristics of the model with equal fore-aft duct incidence settings; $\beta = 0^\circ$.

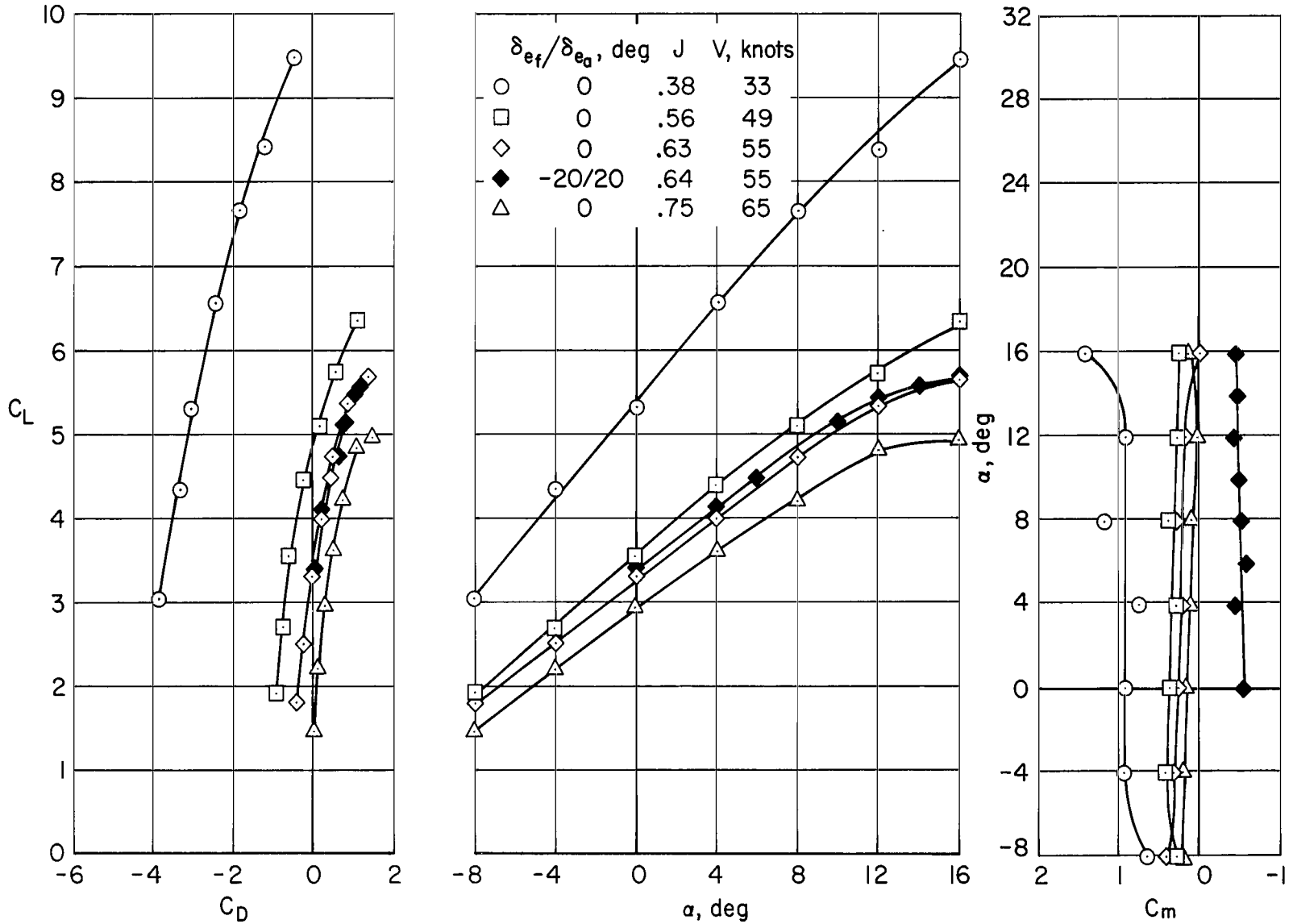

(b) $\delta_D = 30°$

Figure 5.- Continued.

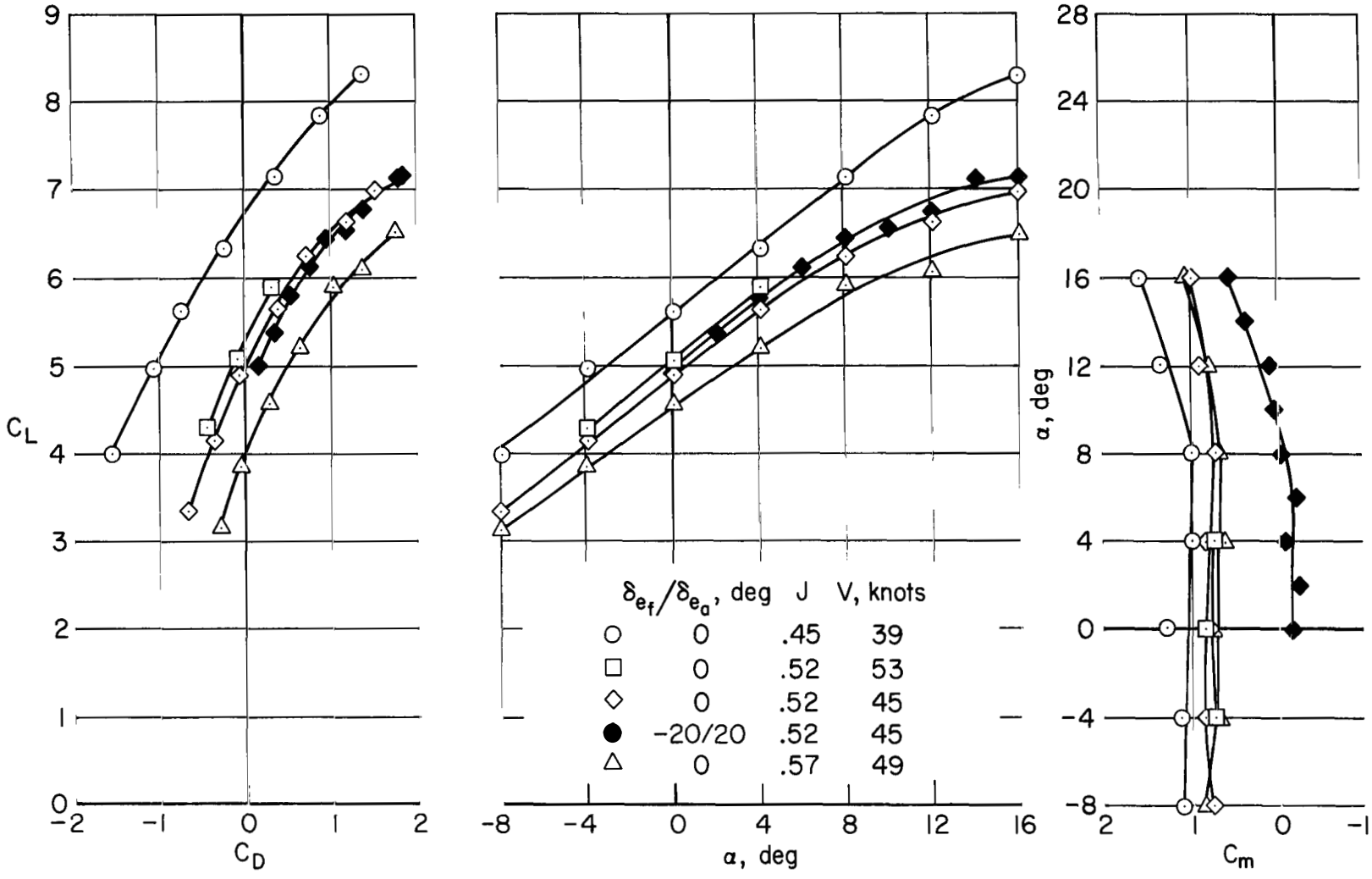

(c) $\delta_D = 40^\circ$

Figure 5.- Continued.

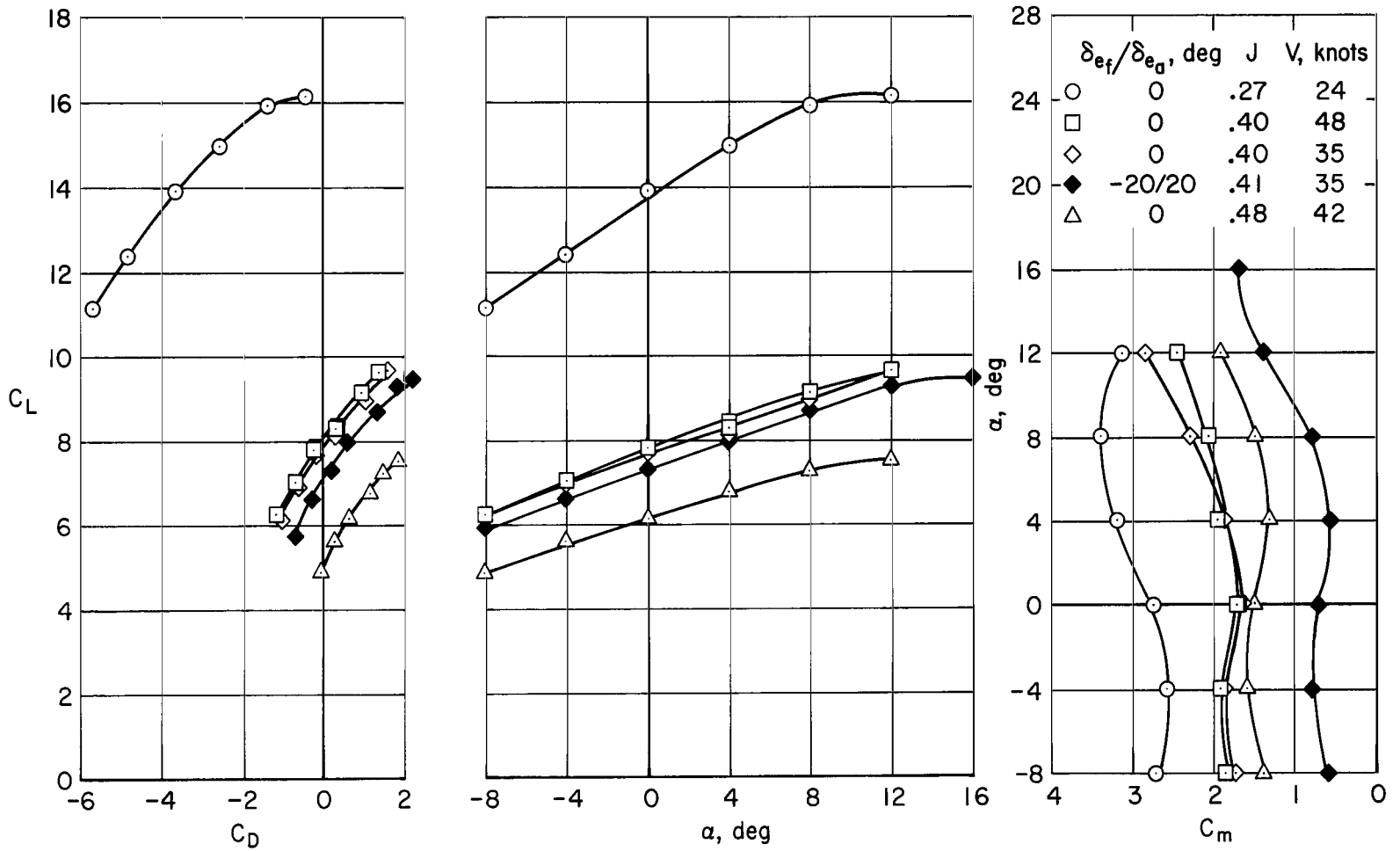

(d) $\delta_D = 50^\circ$

Figure 5.- Continued.

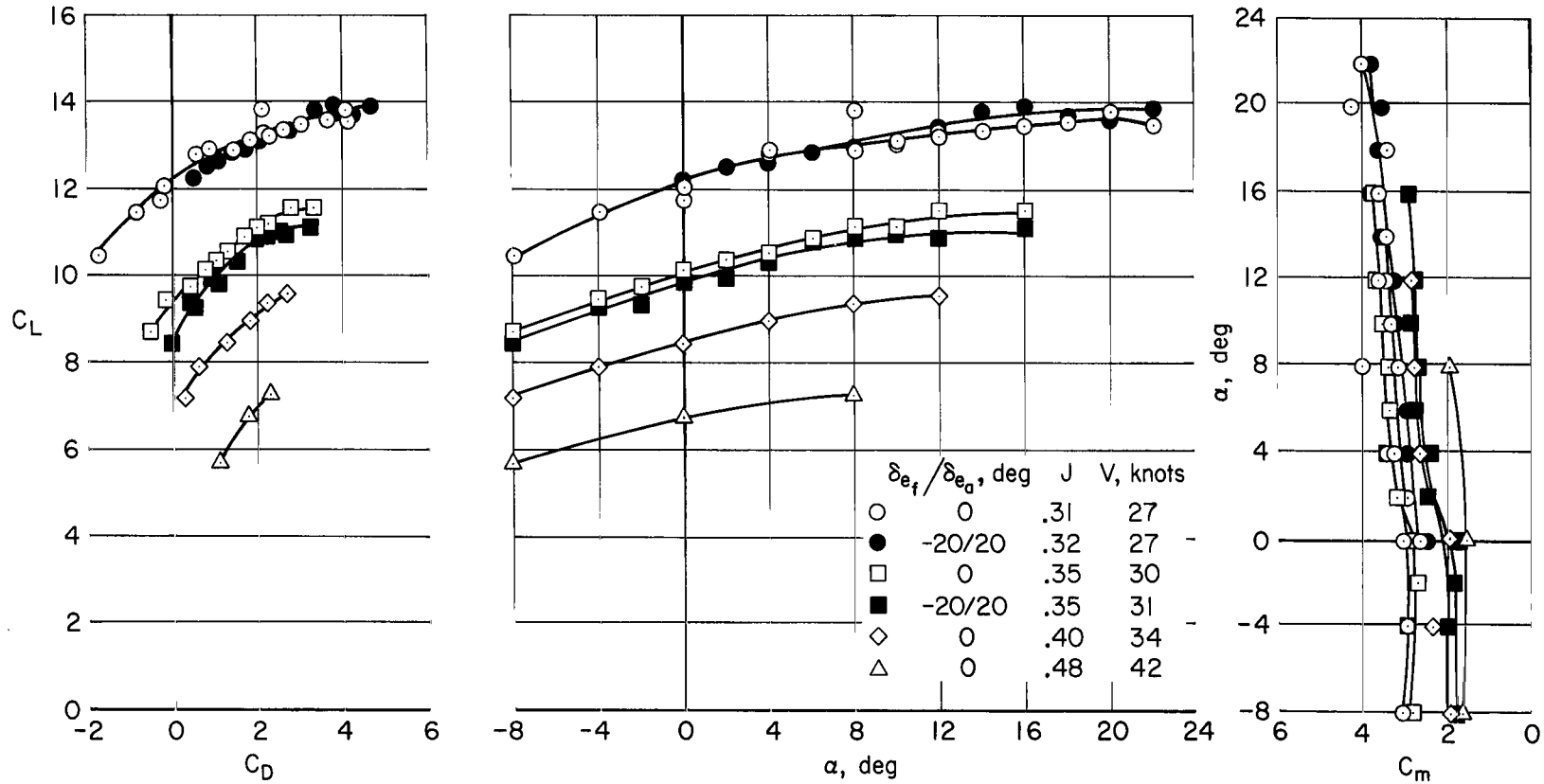

(e) $\delta_D = 60^\circ$

Figure 5.- Continued.

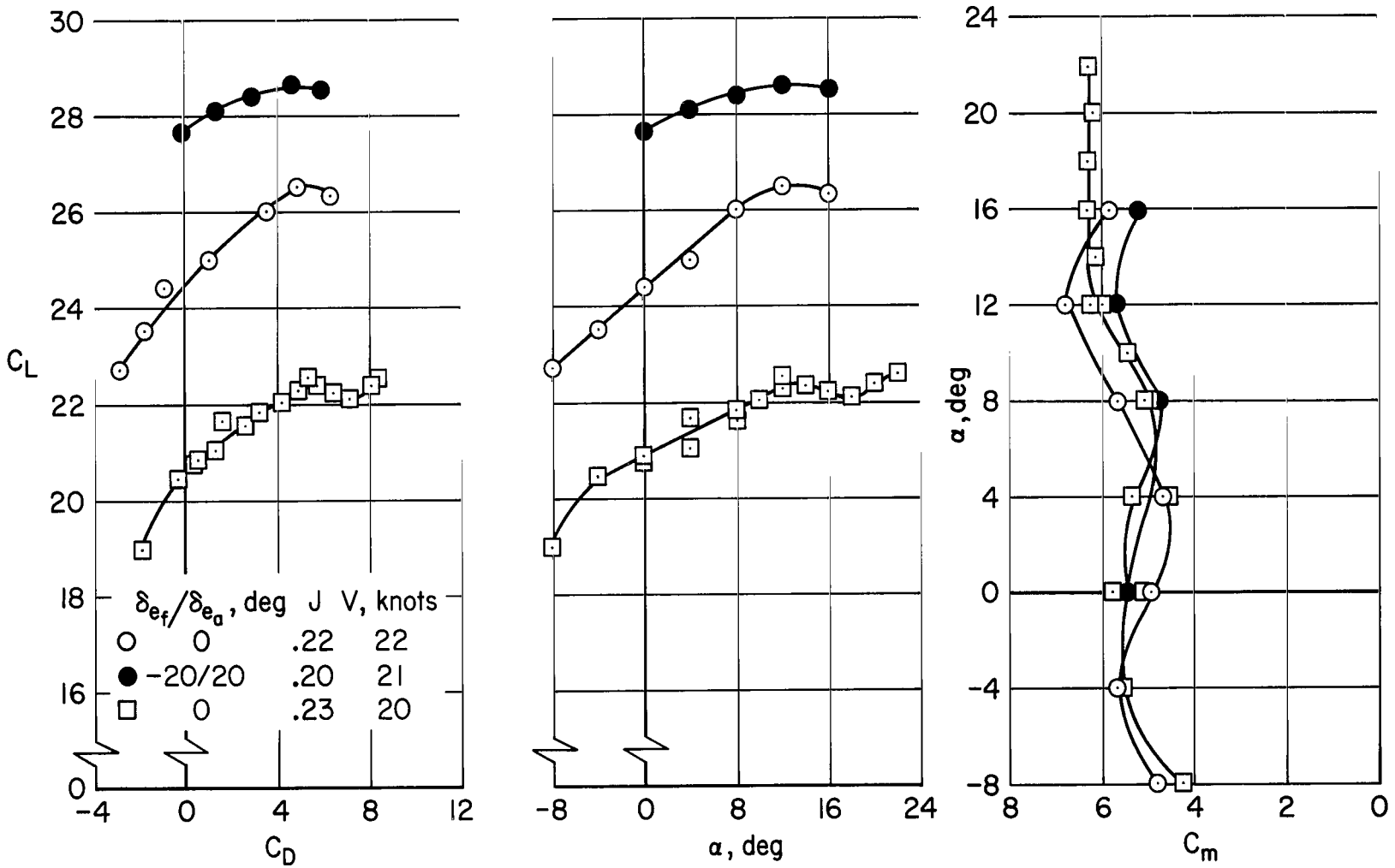

(f) $\delta_D = 70^\circ$

Figure 5.- Continued.

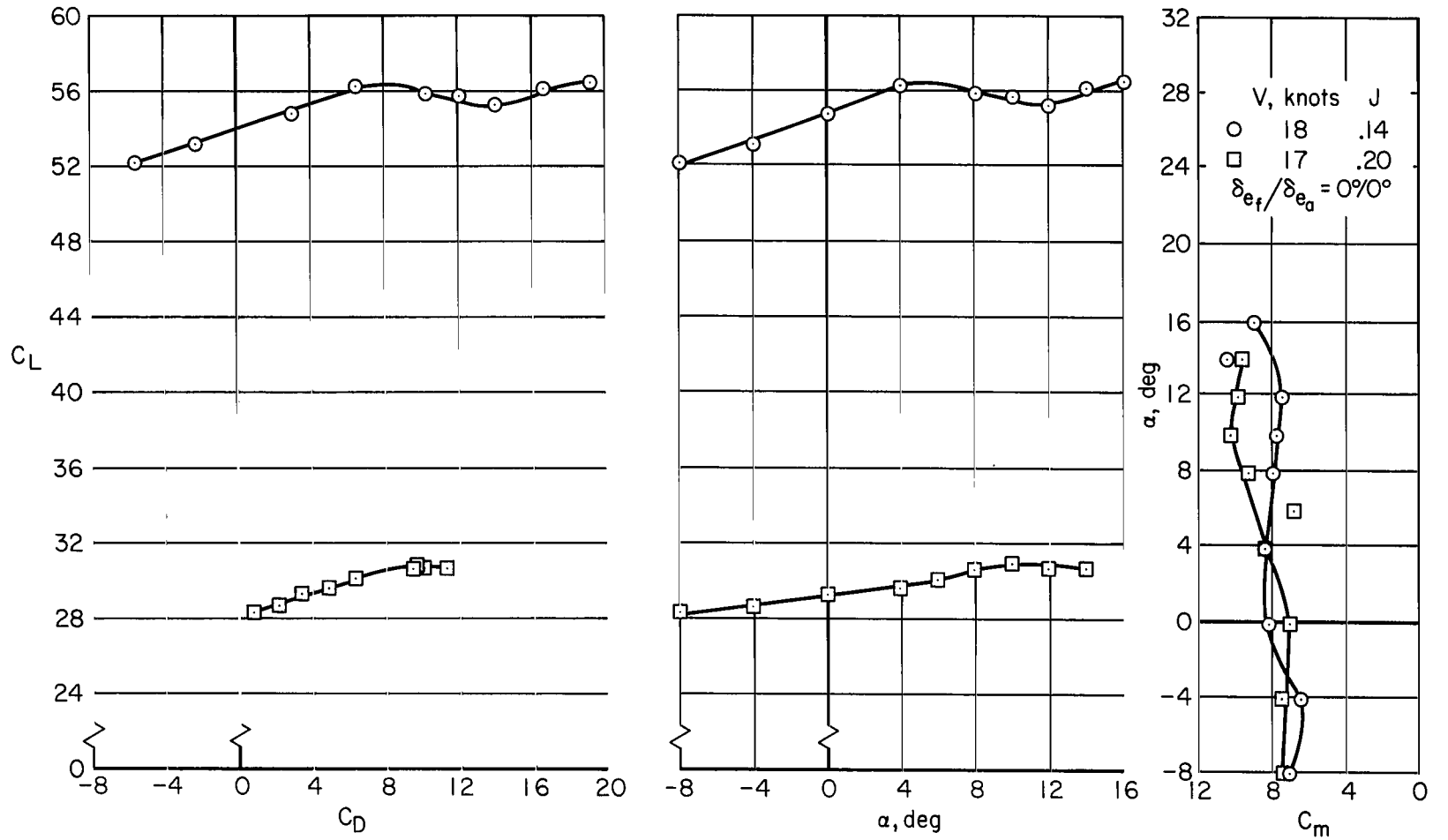

(g) $\delta_D = 80^\circ$

Figure 5.- Concluded.

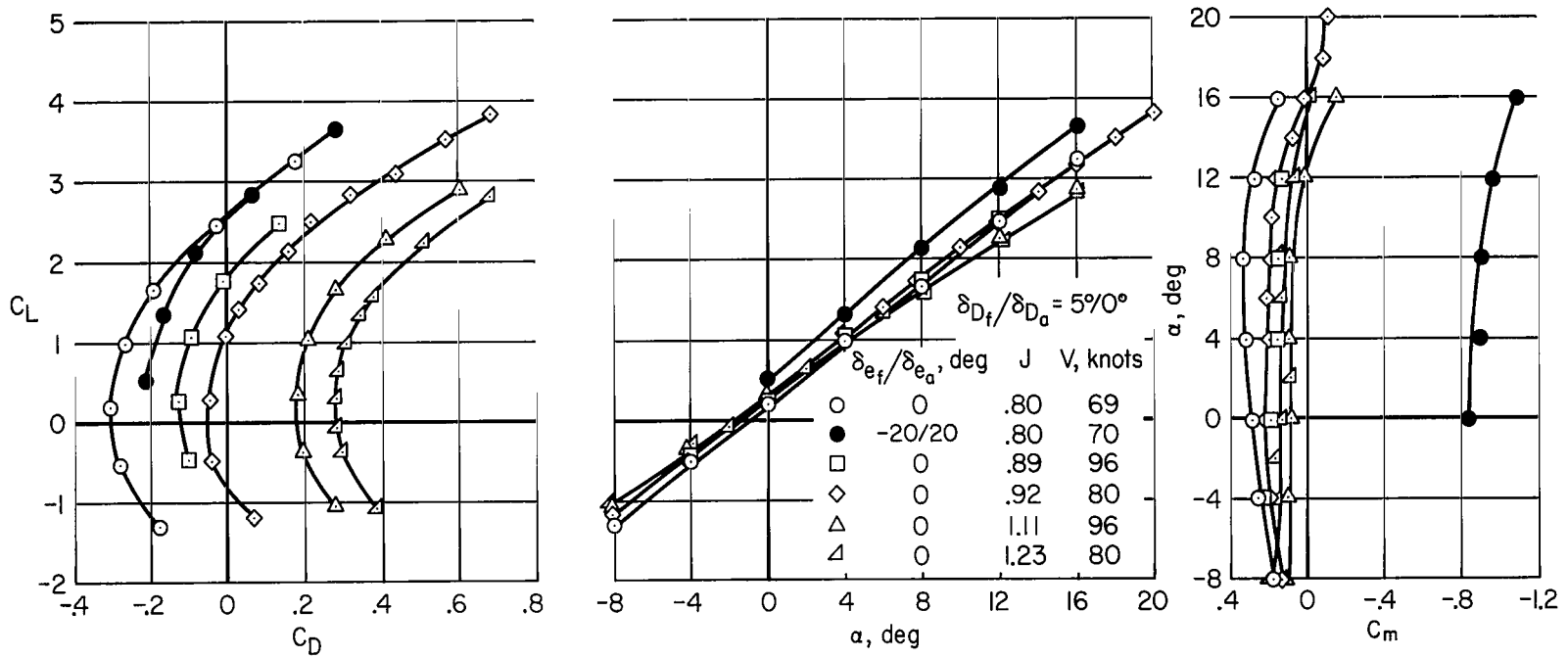

(a) Cruise duct configuration.

Figure 6.- Longitudinal aerodynamic characteristics of the model with differential fore-aft duct incidence settings; $\beta = 0^{\circ}$.

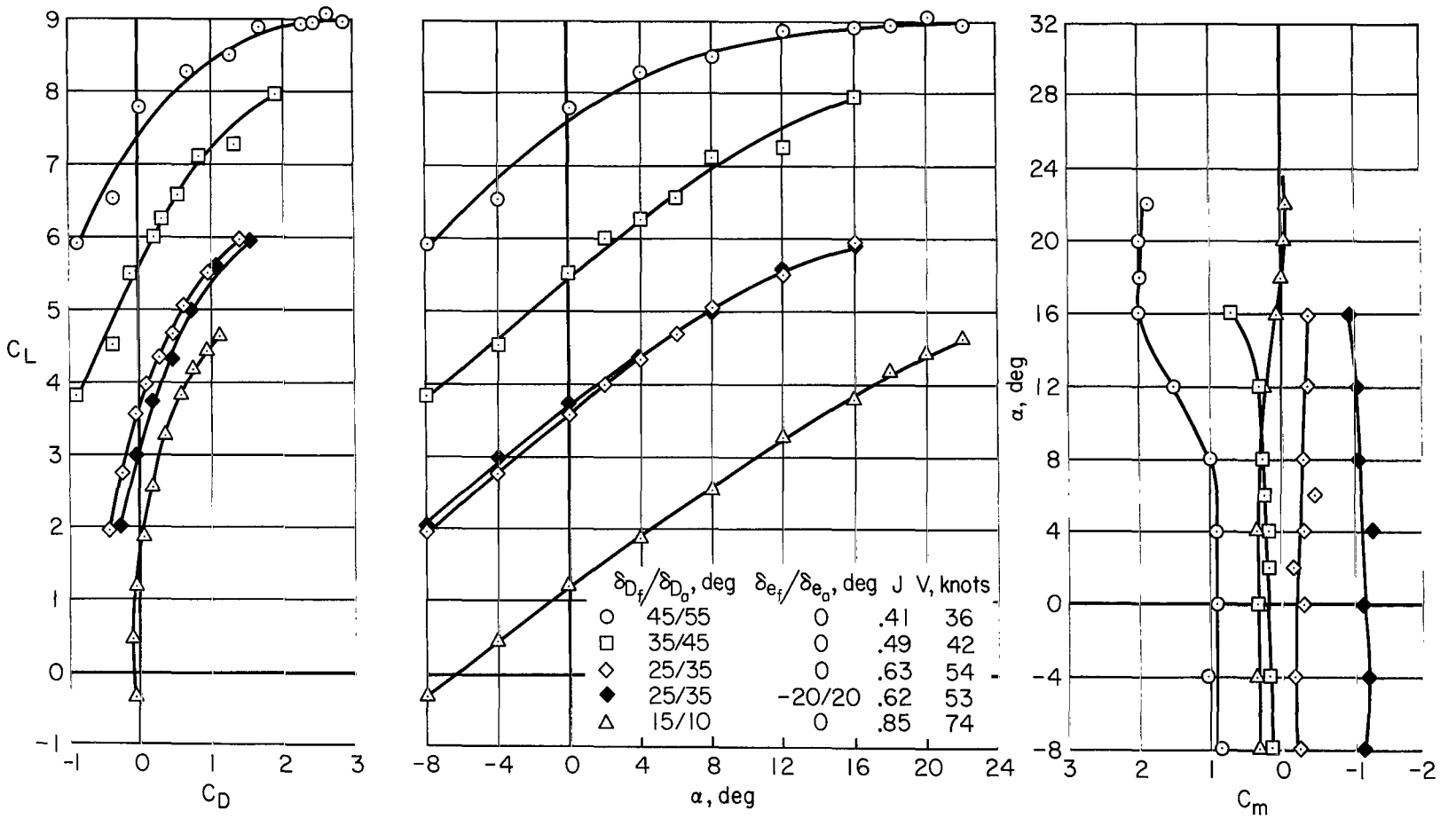

(b) Transition duct configurations.

Figure 6.- Continued.

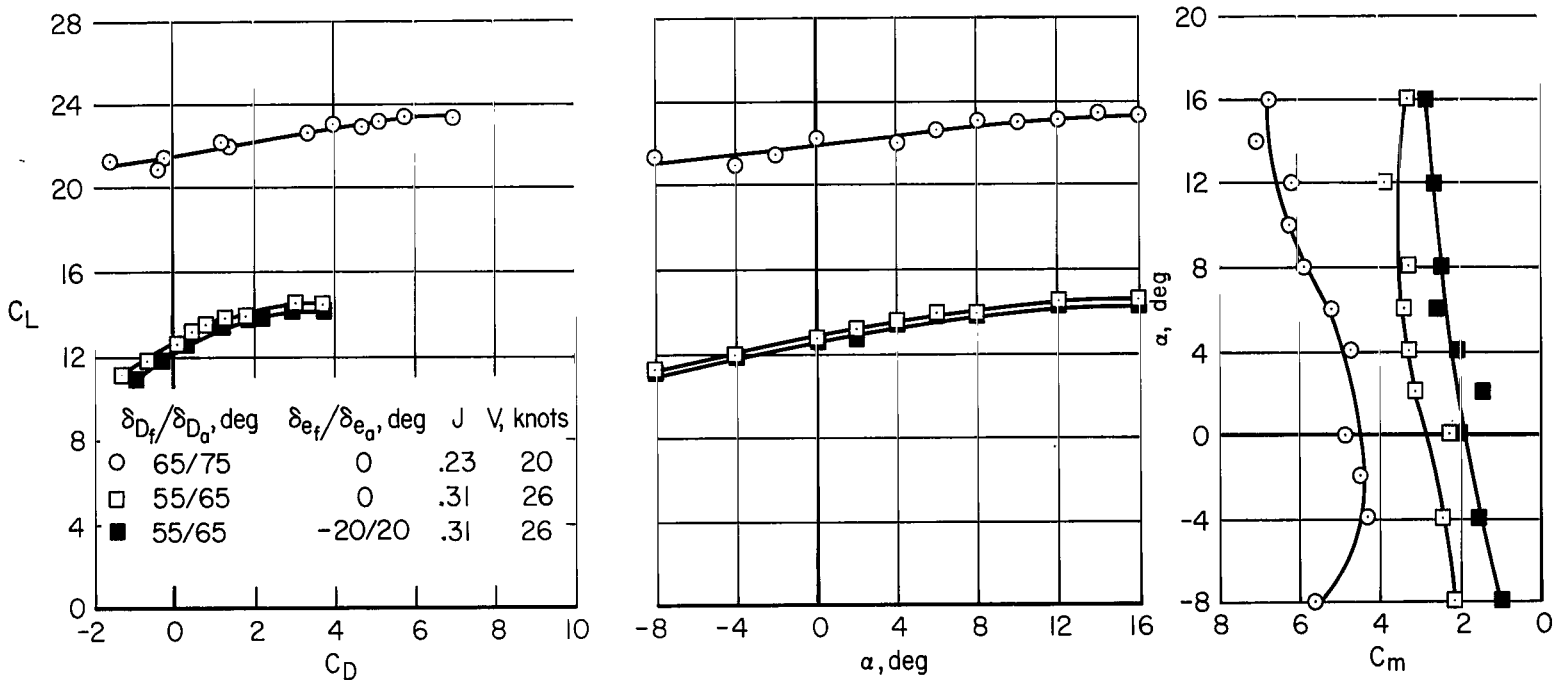

(c) Near-hover duct configurations.

Figure 6.- Concluded.

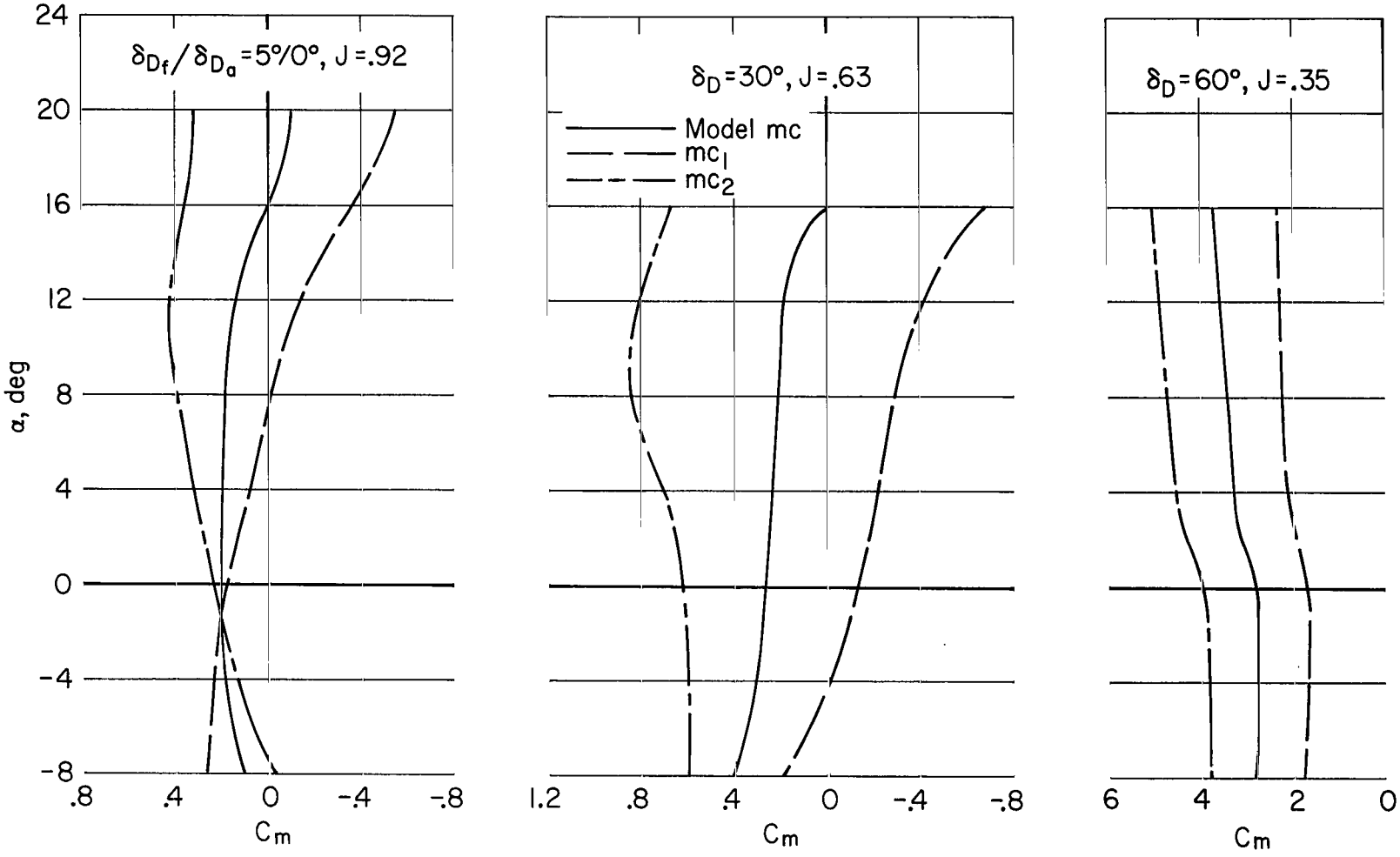

Figure 7.- Static stability of the model for alternate moment centers at several duct incidences; $\beta = 0°$, $\delta_{ef}/\delta_{ea} = 0°/0°$.

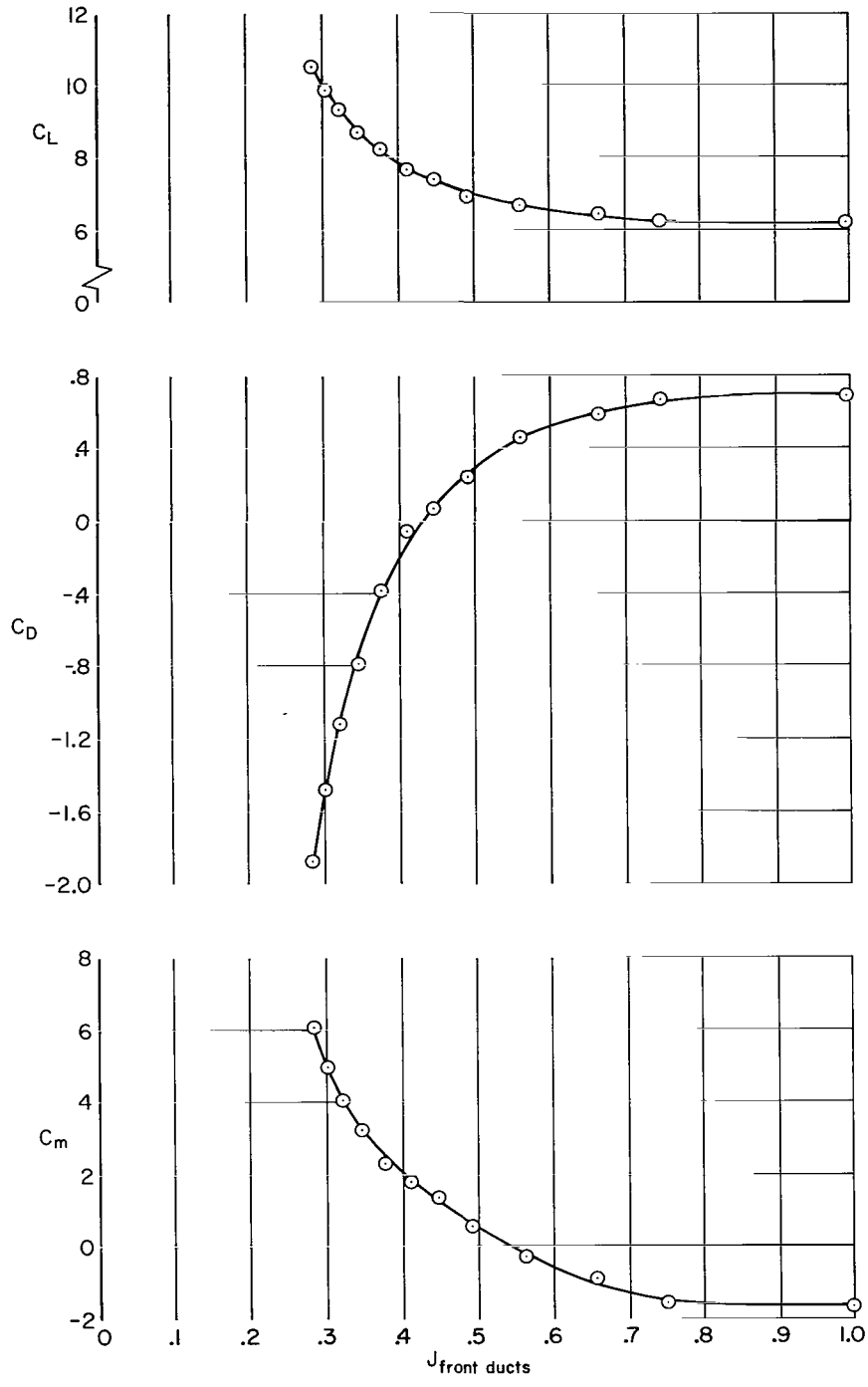

(a) $\delta_D = 50^\circ$, V = 35 knots, $J_{rear\ ducts} = 0.38$.

Figure 8.- Effect of variable front duct thrust on the longitudinal aerodynamic characteristics of the model with the rear duct thrust constant; $\alpha = 0^\circ$, $\beta = 0^\circ$, $\delta_{e_f}/\delta_{e_a} = 0^\circ/0^\circ$.

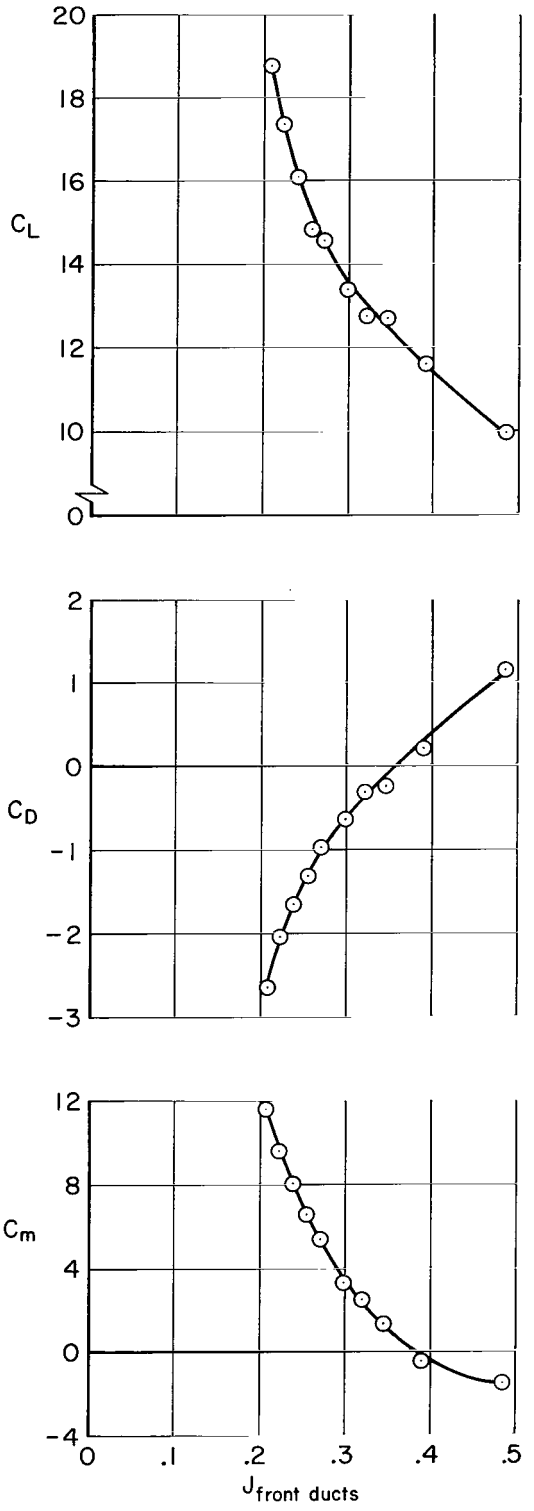

(b) $\delta_D = 60^\circ$, V = 26 knots, $J_{rear\ ducts} = 0.27$.

Figure 8.- Continued.

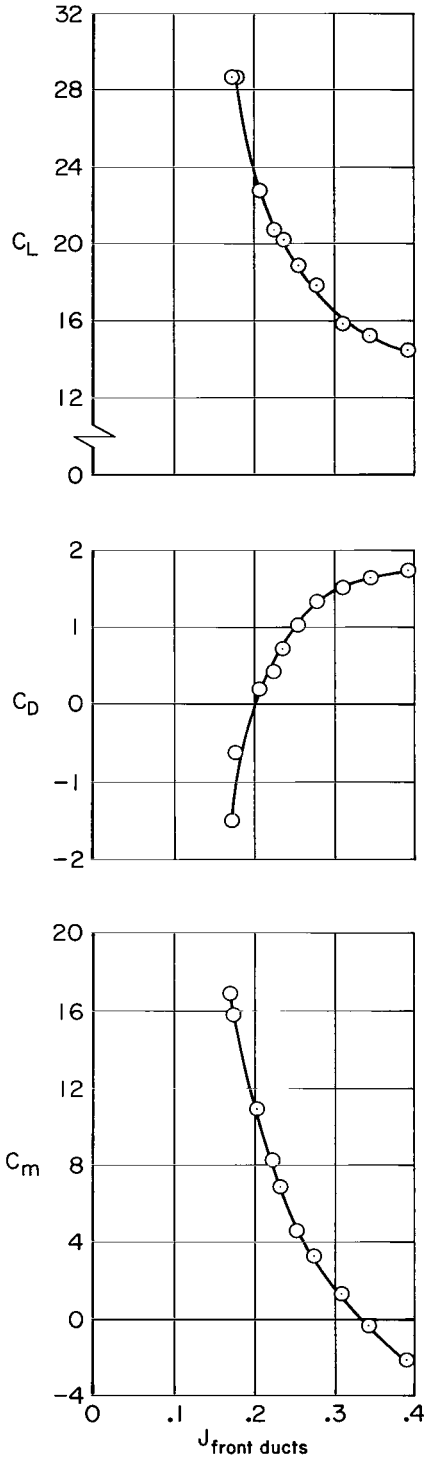

(c) $\delta_D = 70^\circ$, V = 22 knots, $J_{rear\ ducts} = 0.25$.

Figure 8.- Continued.

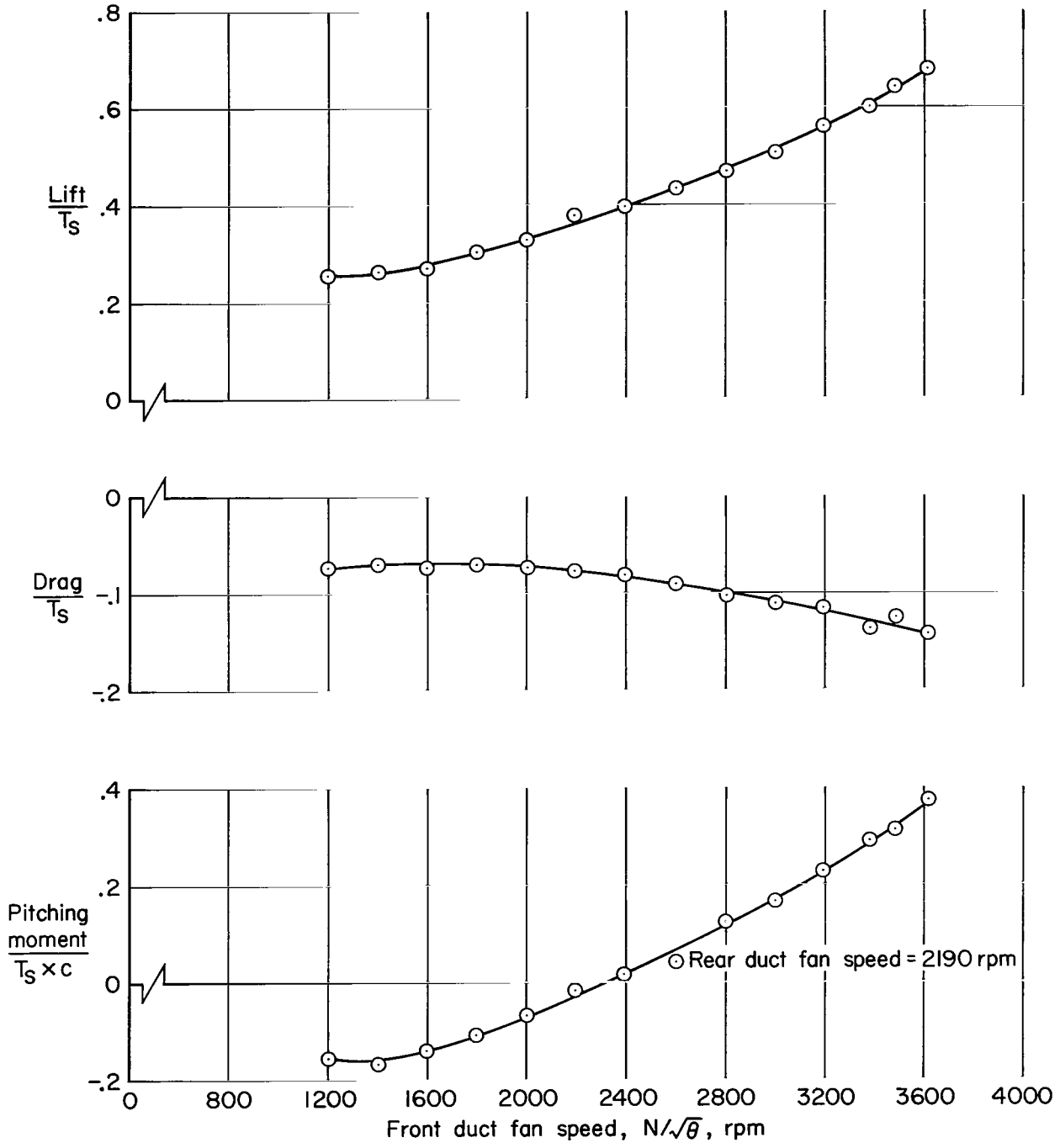

(d) $\delta_D = 80^\circ$, V = 0 knots

Figure 8.- Concluded.

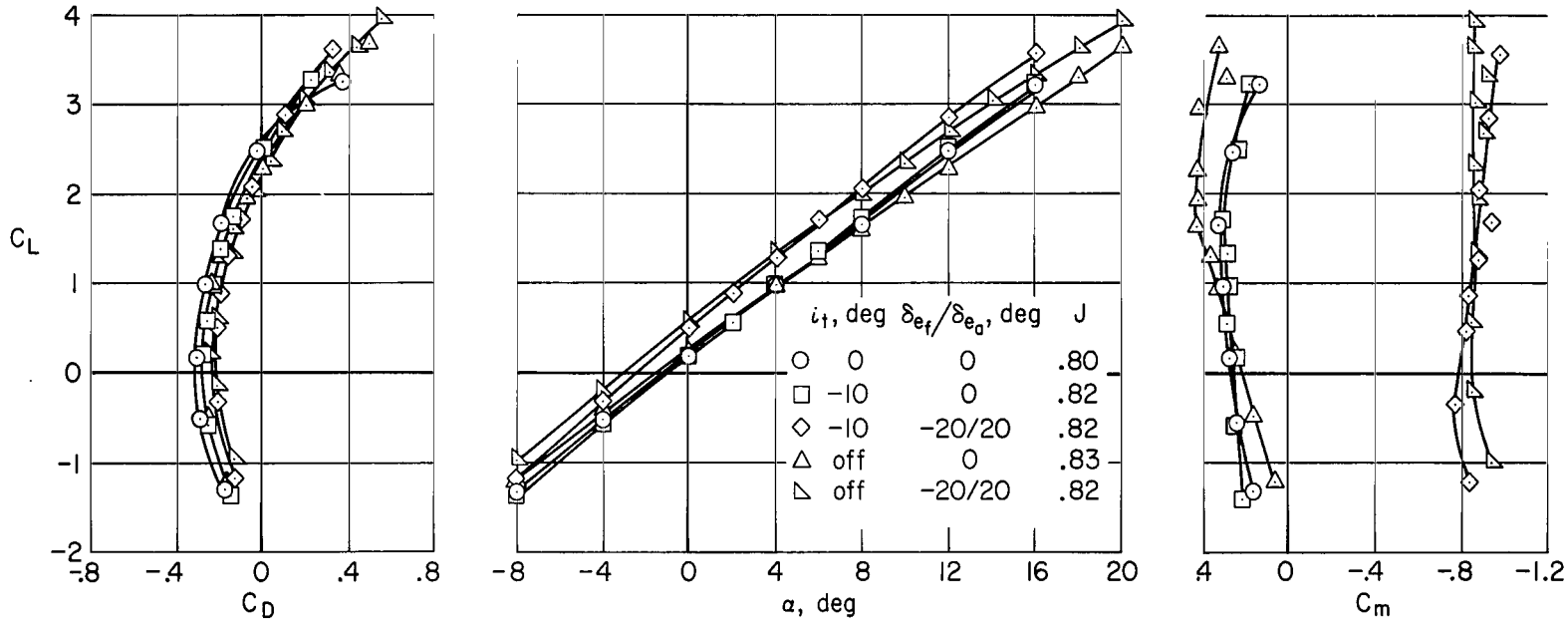

(a) $\delta_{D_f}/\delta_{D_a} = 5^\circ/0^\circ$, V = 70 knots

Figure 9.- Effect on the model longitudinal aerodynamic characteristics of wing tips outboard of the rear ducts; $\beta = 0^\circ$.

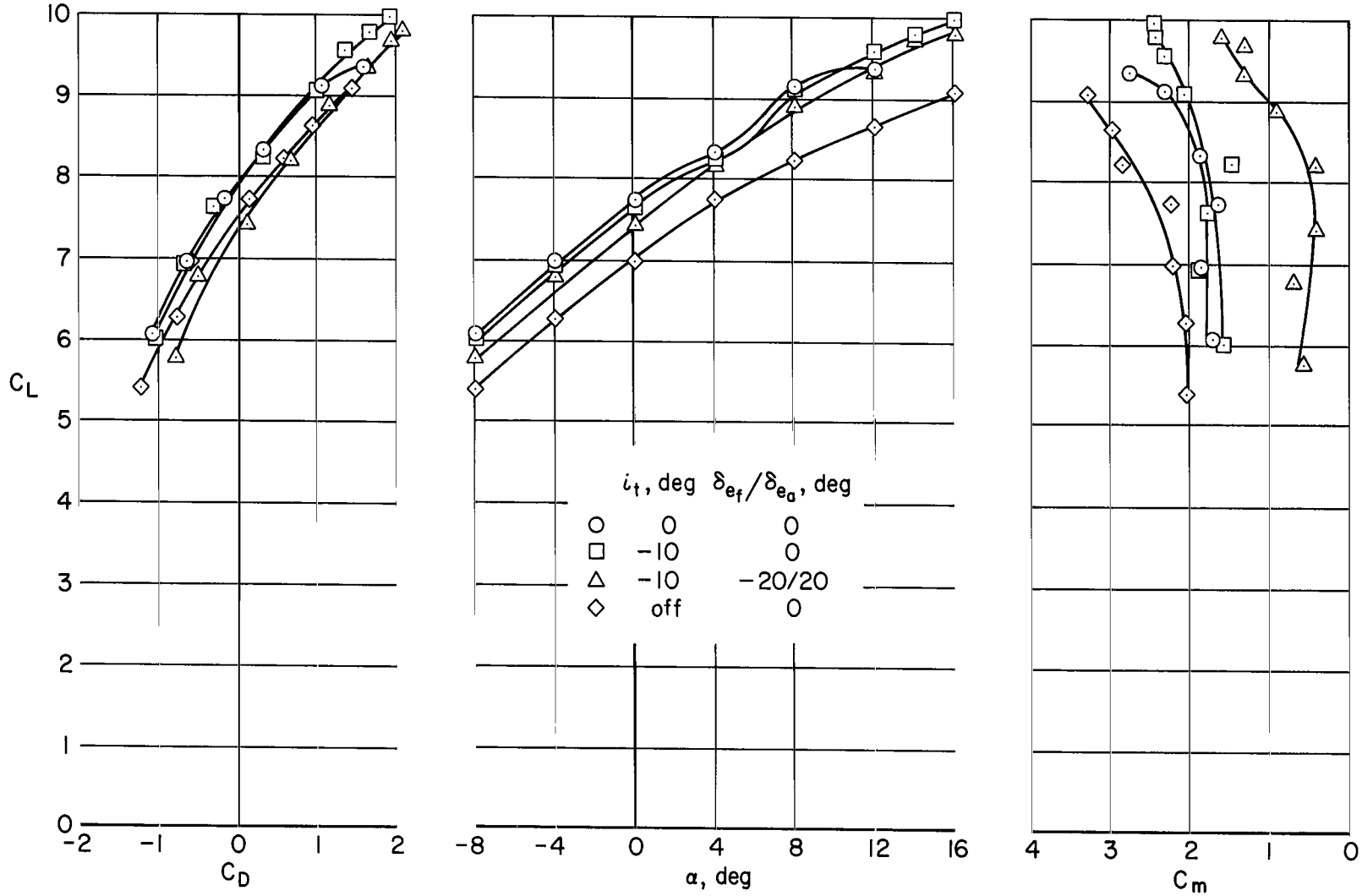

(b) $\delta_D = 50^\circ$, J = 0.41, V = 35 knots

Figure 9.- Concluded.

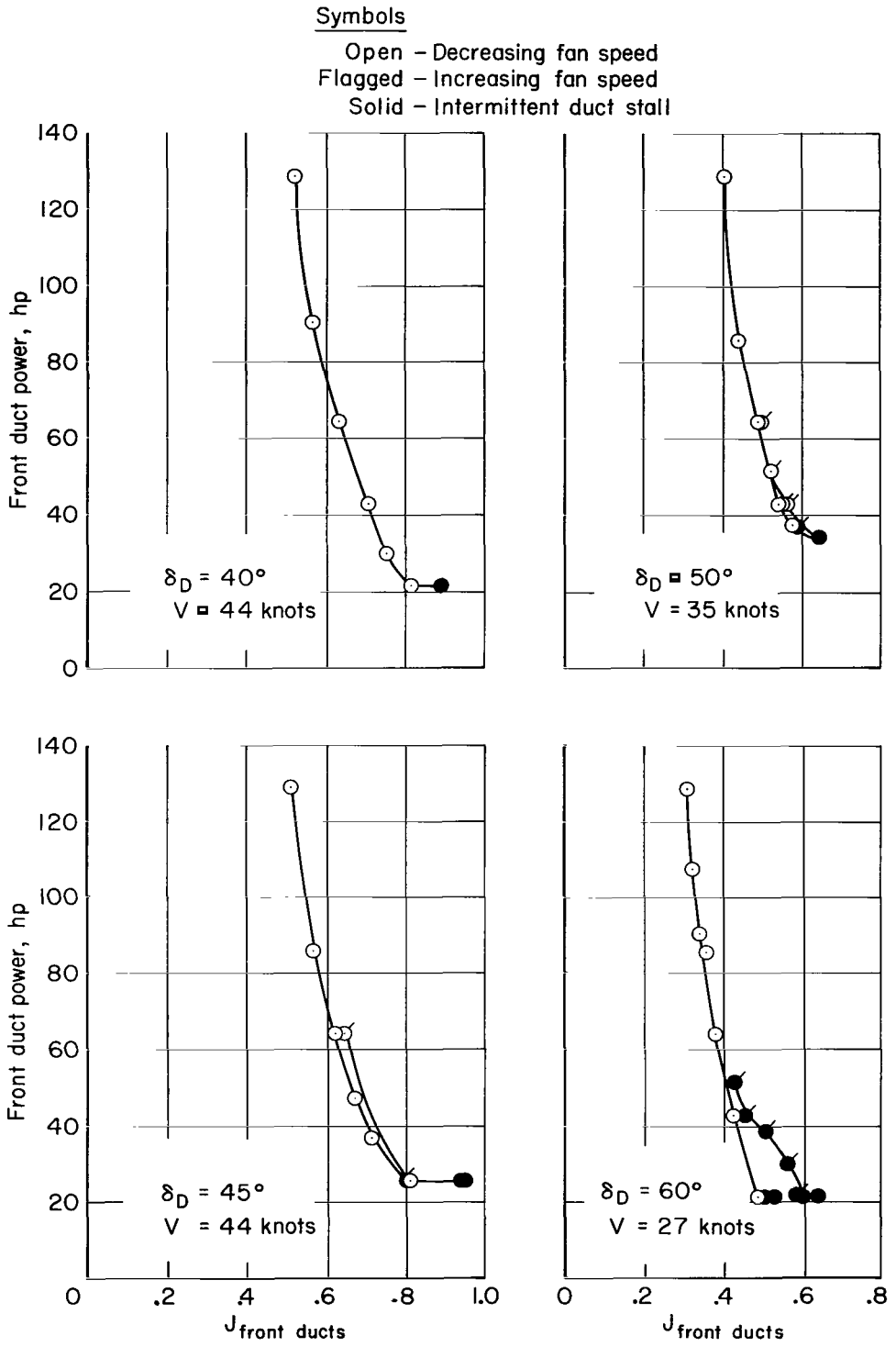

Figure 10.- Variation of input power with front duct fan speed showing front duct stall; $\alpha = 0^\circ$, $\beta = 0^\circ$, $\delta_{ef}/\delta_{ea} = 0^\circ/0^\circ$.

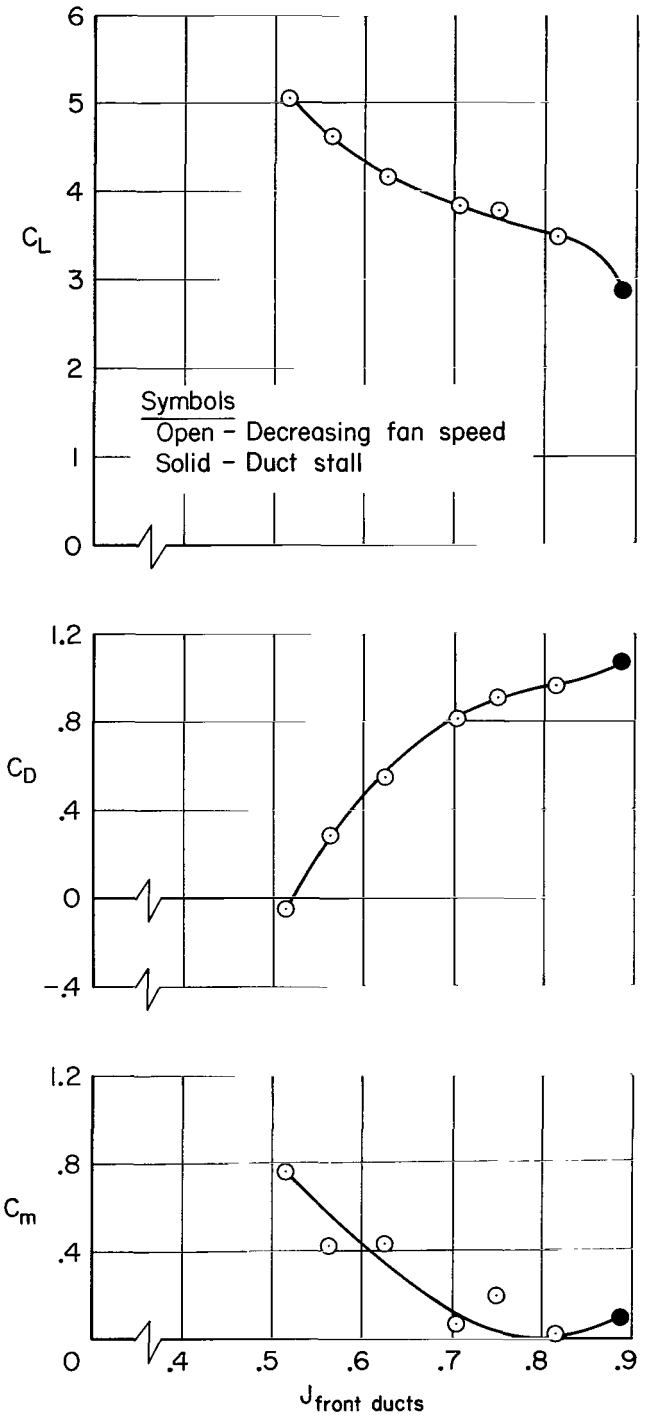

(a) $\delta_D = 40^\circ$, V = 44 knots

Figure 11.- Effect of front duct stall on the model longitudinal aerodynamic characteristics. Front and rear duct fan speeds varied simultaneously until front ducts stalled; $\alpha = 0^\circ$, $\beta = 0^\circ$, $\delta_{e_f}/\delta_{e_a} = 0^\circ/0^\circ$.

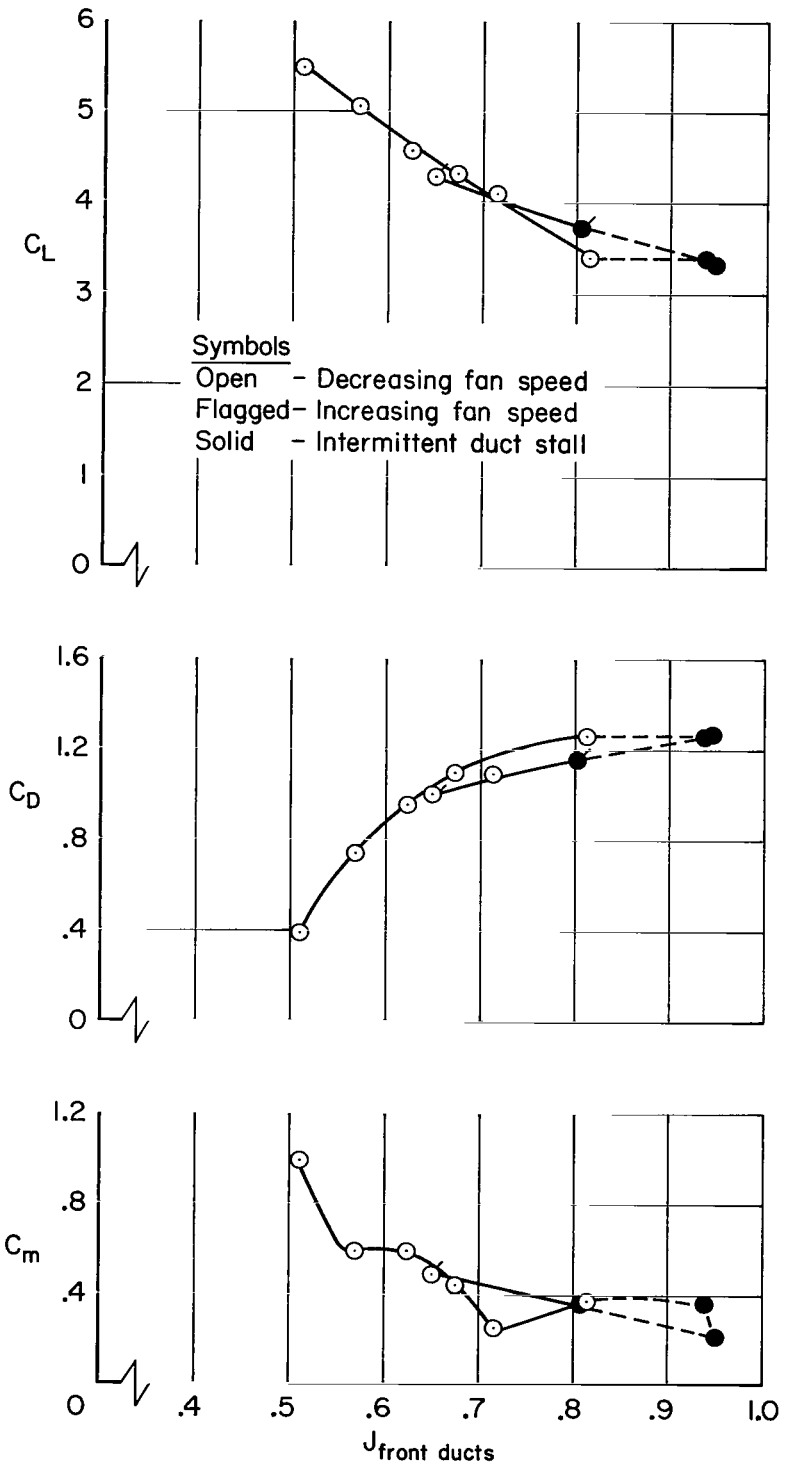

(b) $\delta_D = 45^\circ$, V = 44 knots

Figure 11.- Continued.

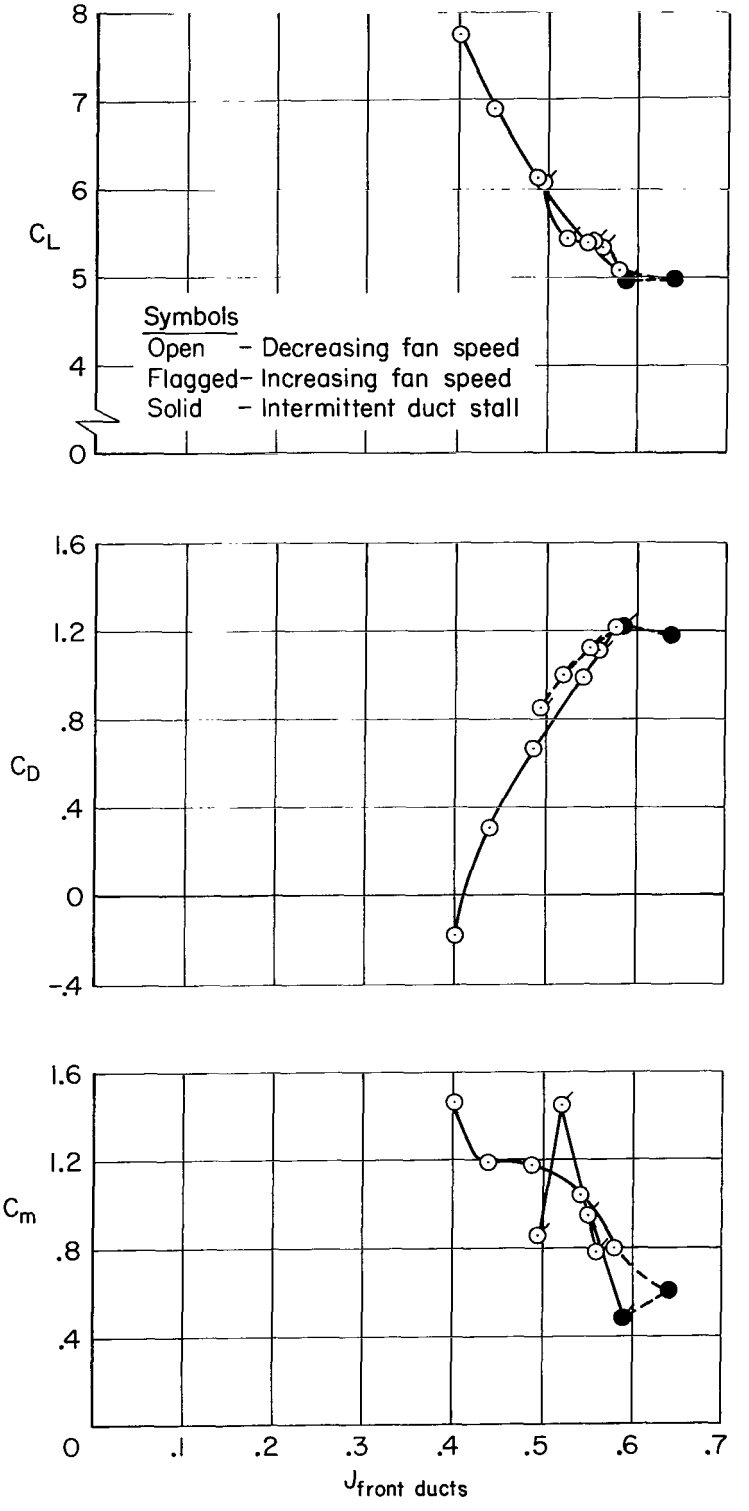

(c) $\delta_D = 50^\circ$, V = 35 knots

Figure 11.- Continued.

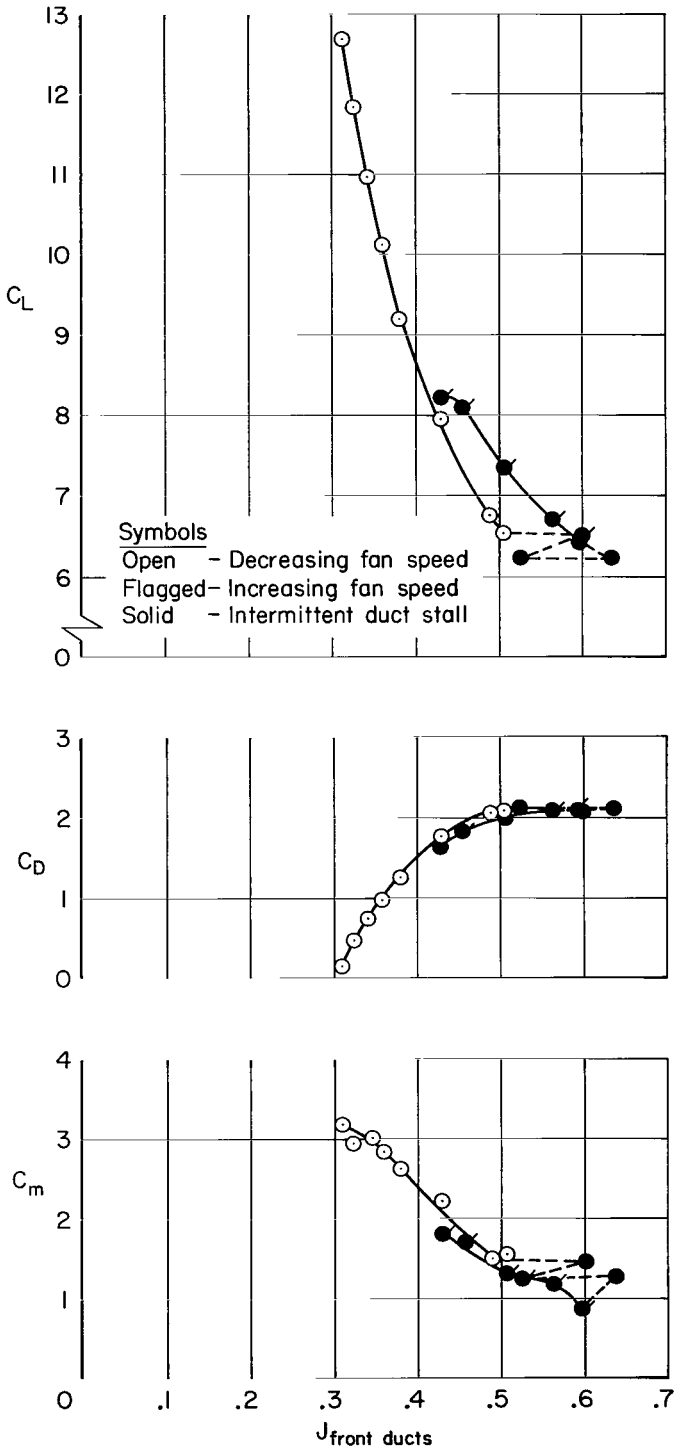

(d) $\delta_D = 60^\circ$, V = 27 knots

Figure 11.- Concluded.

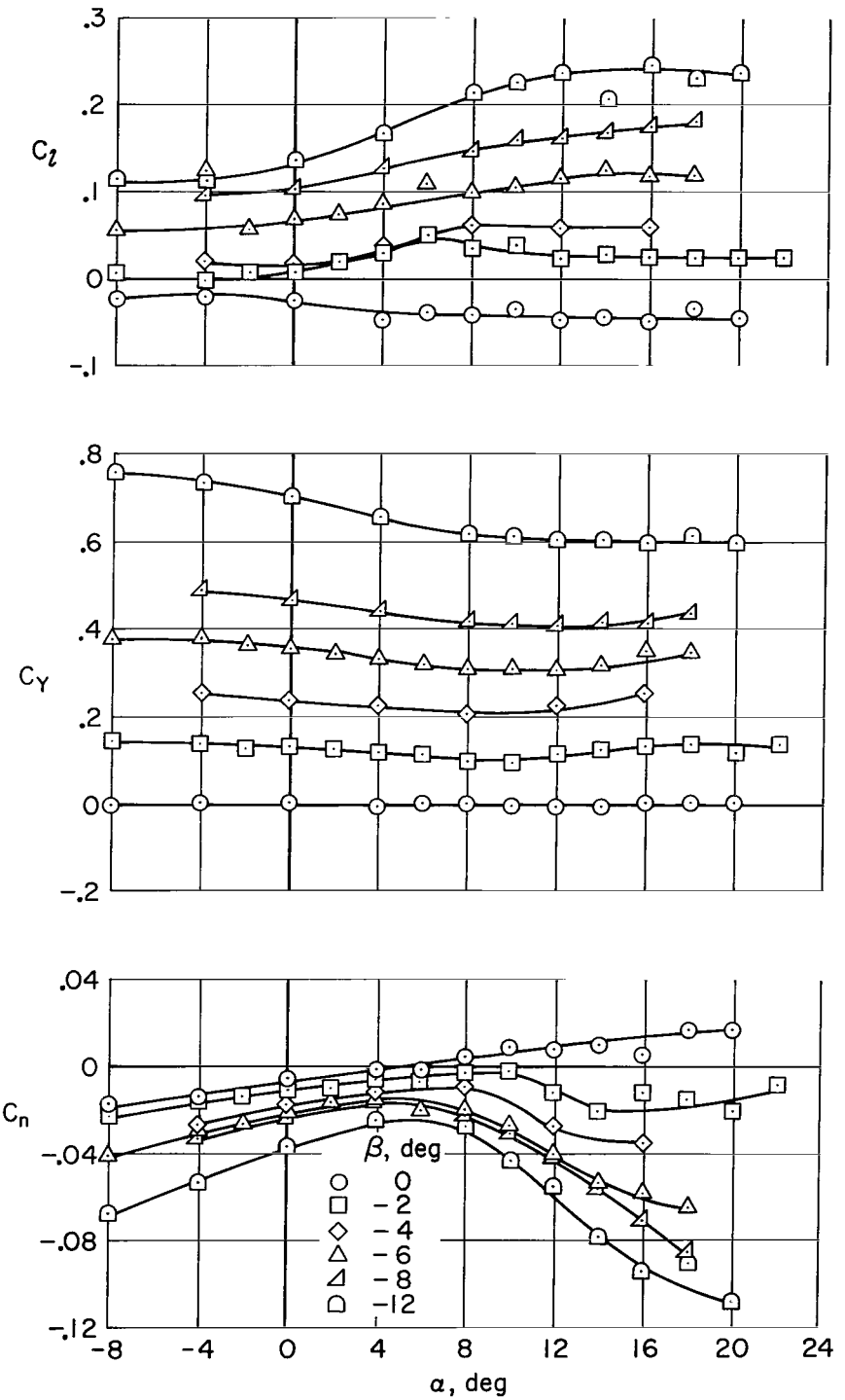

(a) $\delta_{D_f}/\delta_{D_a}$ = 5°/0°, J = 0.94, V = 80 knots

Figure 12.- Lateral-directional aerodynamic characteristics of the model at sideslip; $\delta_{a_l}/\delta_{a_r}$ = 0°/0°.

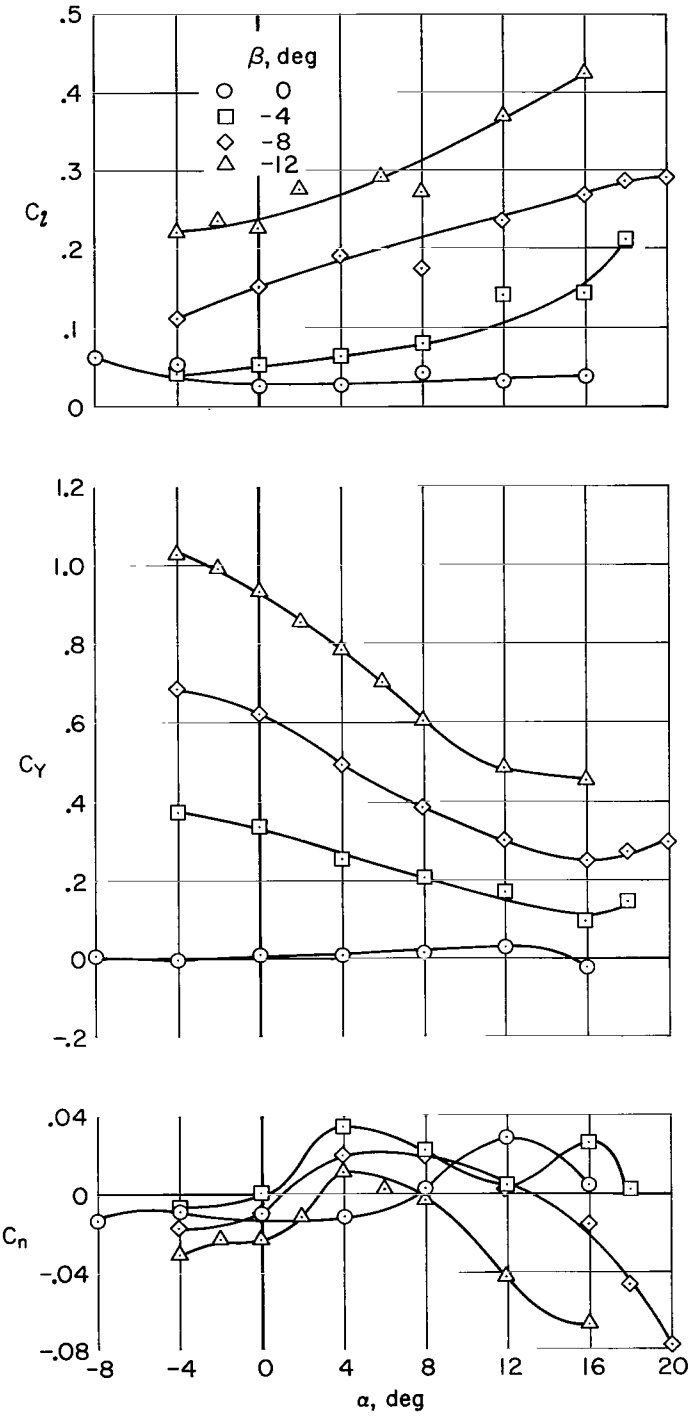

(b) $\delta_D = 30^\circ$, J = 0.64, V = 55 knots

Figure 12.- Continued.

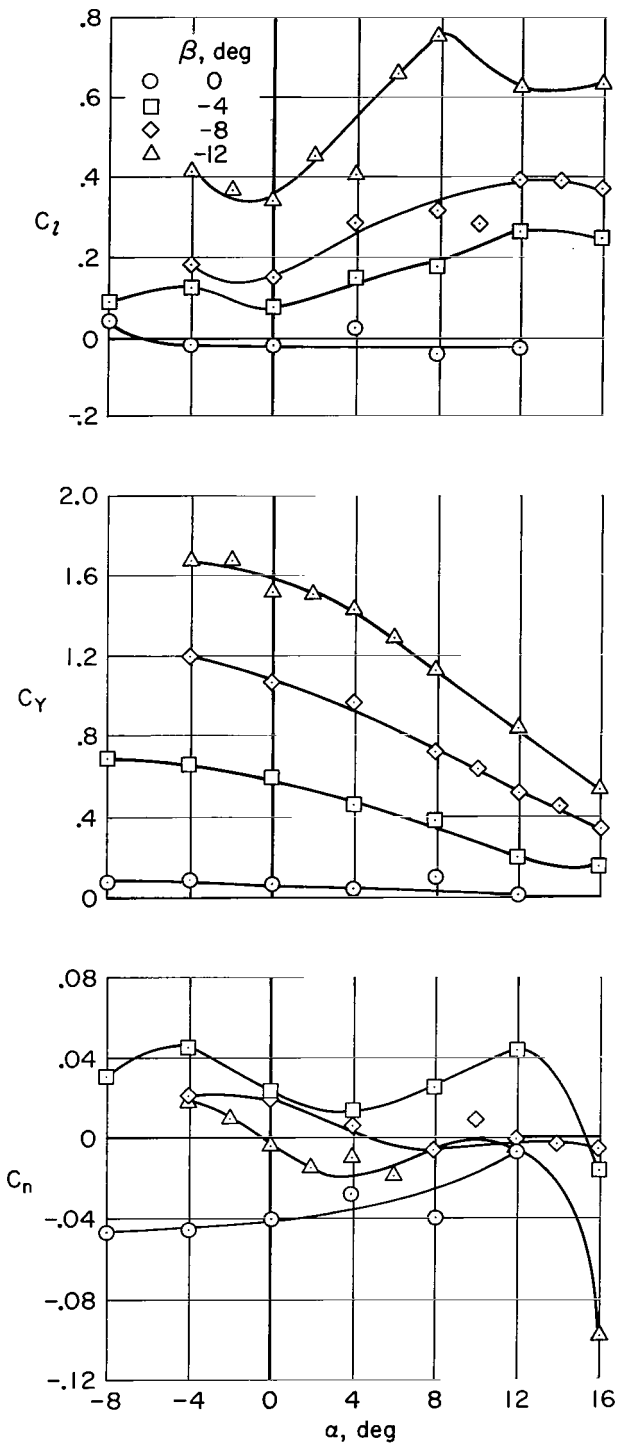

(c) $\delta_D = 50^\circ$, J = 0.40, V = 35 knots

Figure 12.- Concluded.

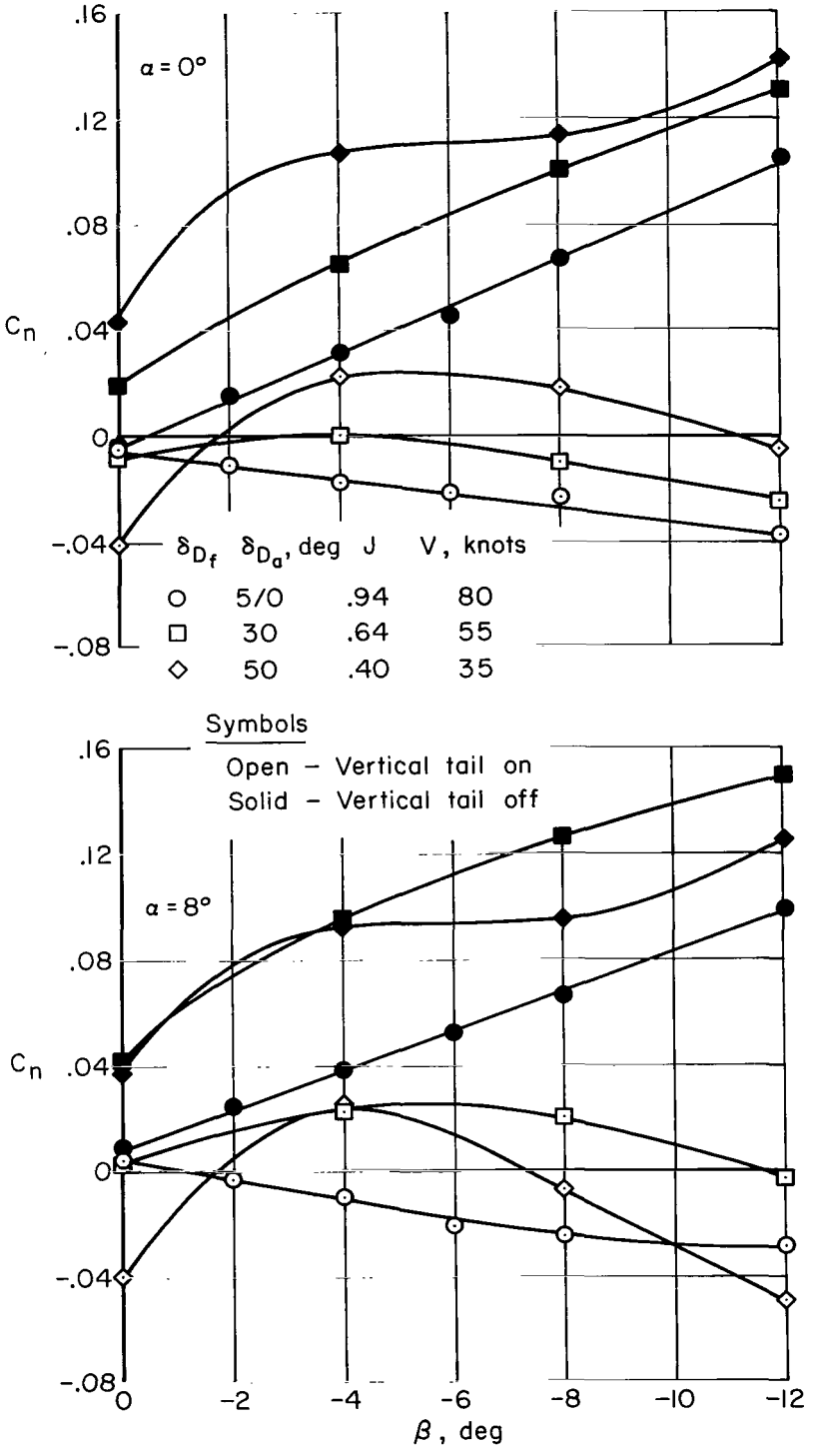

Figure 13.- Vertical-tail contribution to directional stability; $\delta_{a_l}/\delta_{a_r} = 0°/0°$.

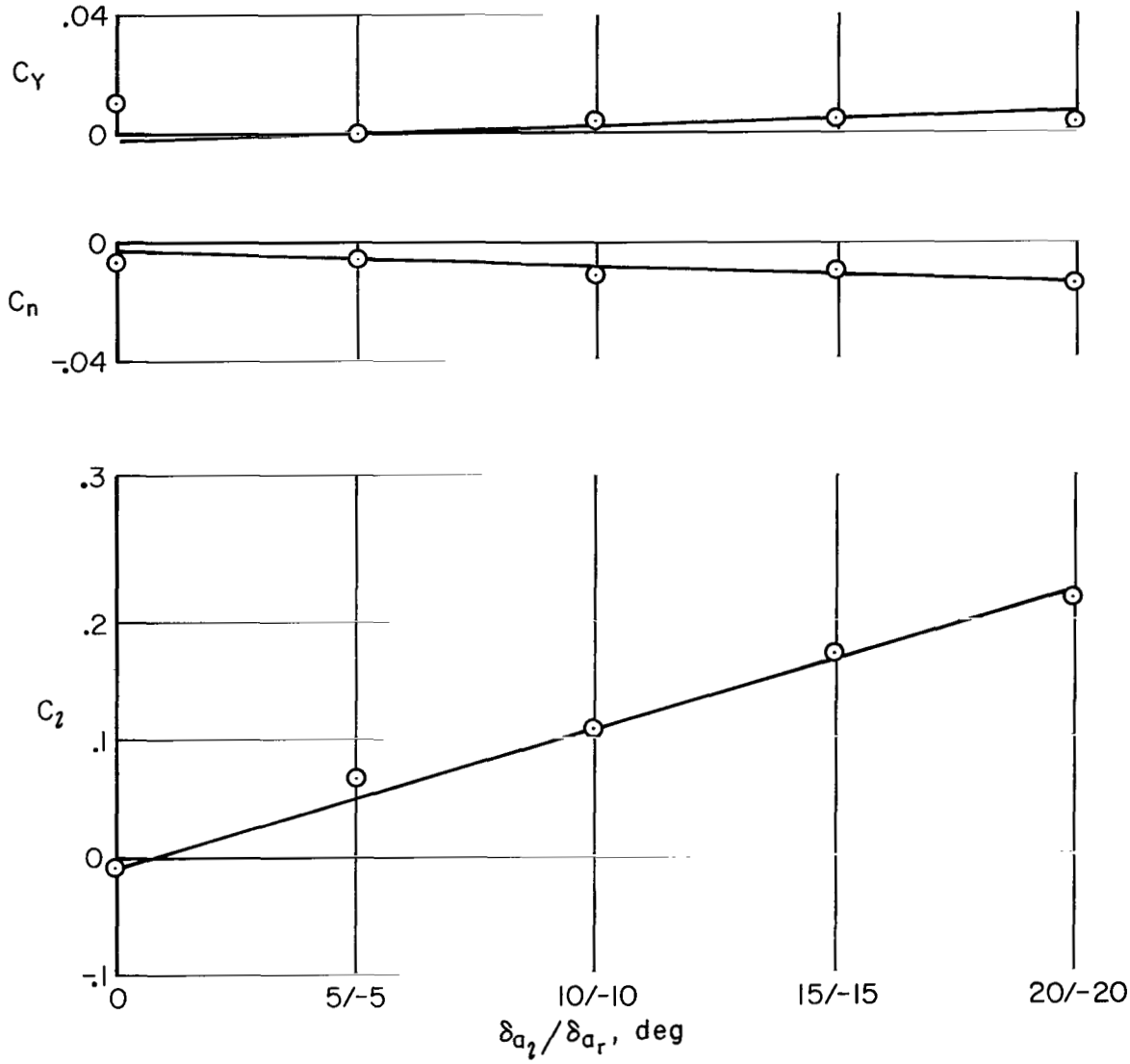

(a) $\delta_{D_f}/\delta_{D_a} = 5^\circ/0^\circ$, J = 0.93, V = 80 knots

Figure 14.- Effect of differential left-right duct exit vane deflection on the model lateral-directional aerodynamic characteristics; $\alpha = 0^\circ$, $\beta = 0^\circ$.

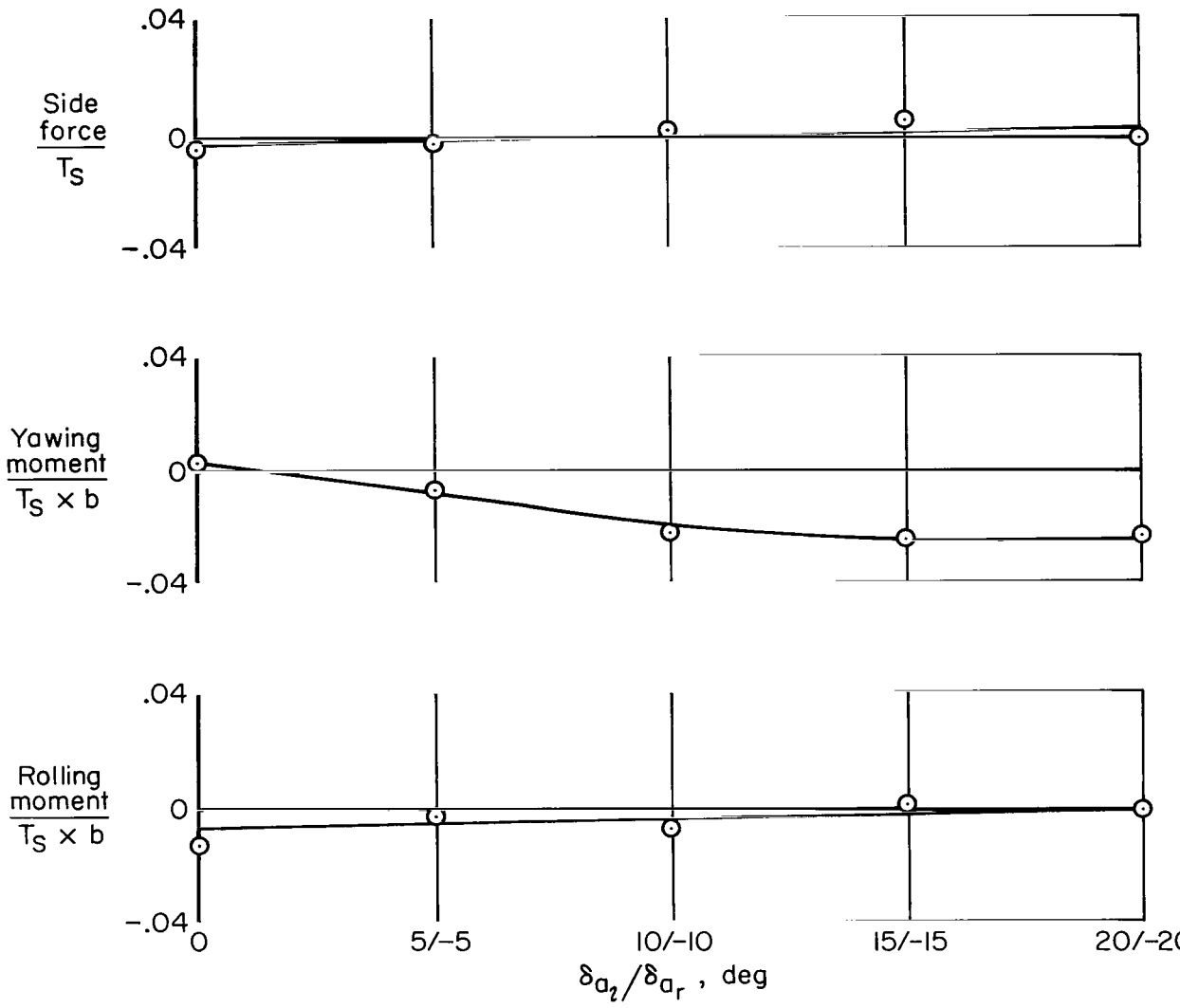

(b) $\delta_D = 80^\circ$, V = 0, N = 2190 rpm

Figure 14.- Concluded.

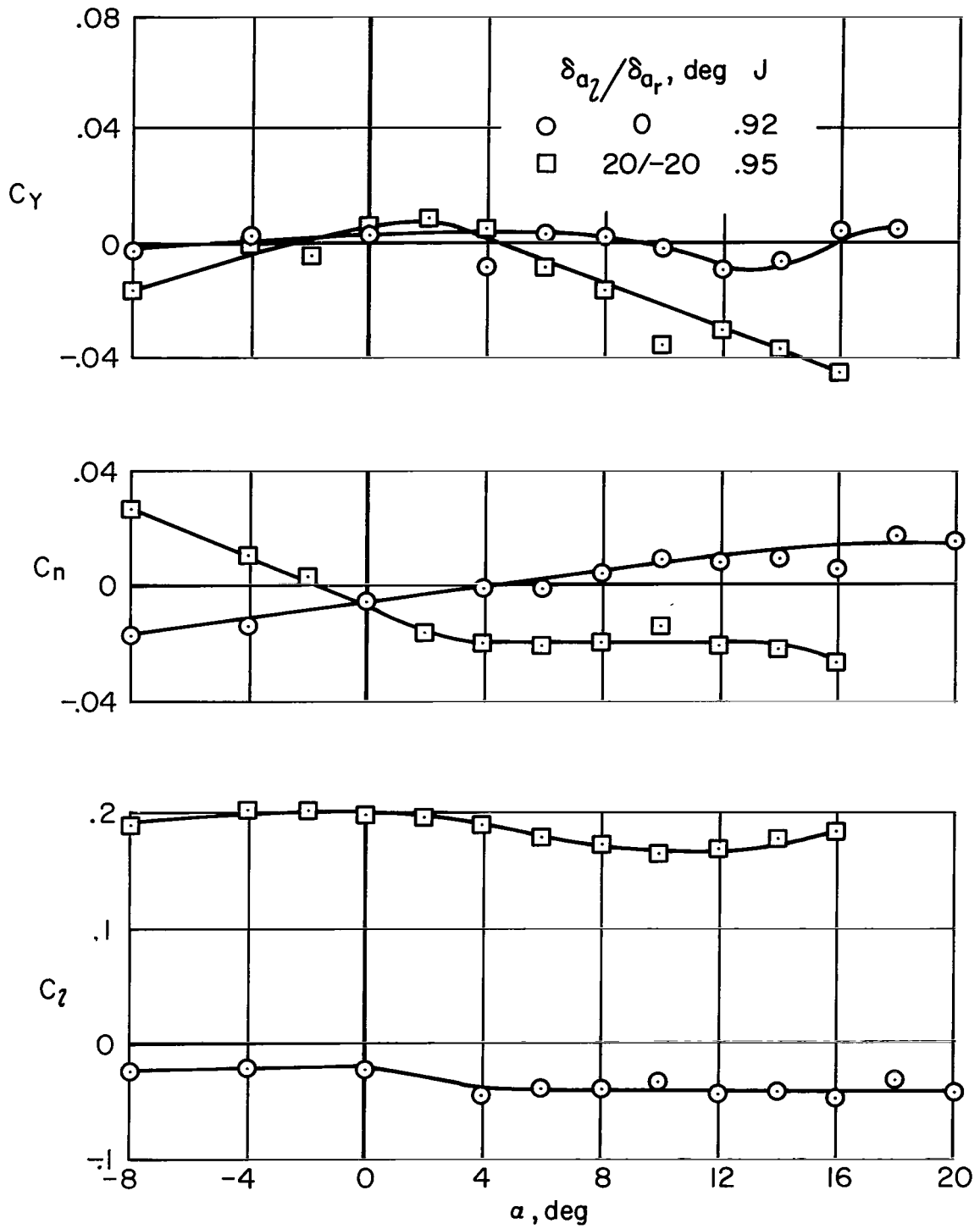

(a) $\delta_{D_f}/\delta_{D_a}$ = 5°/0°, V = 80 knots, β = 0°

Figure 15.- Lateral-directional aerodynamic characteristics of the model with the duct exit vanes undeflected and differentially deflected left and right.

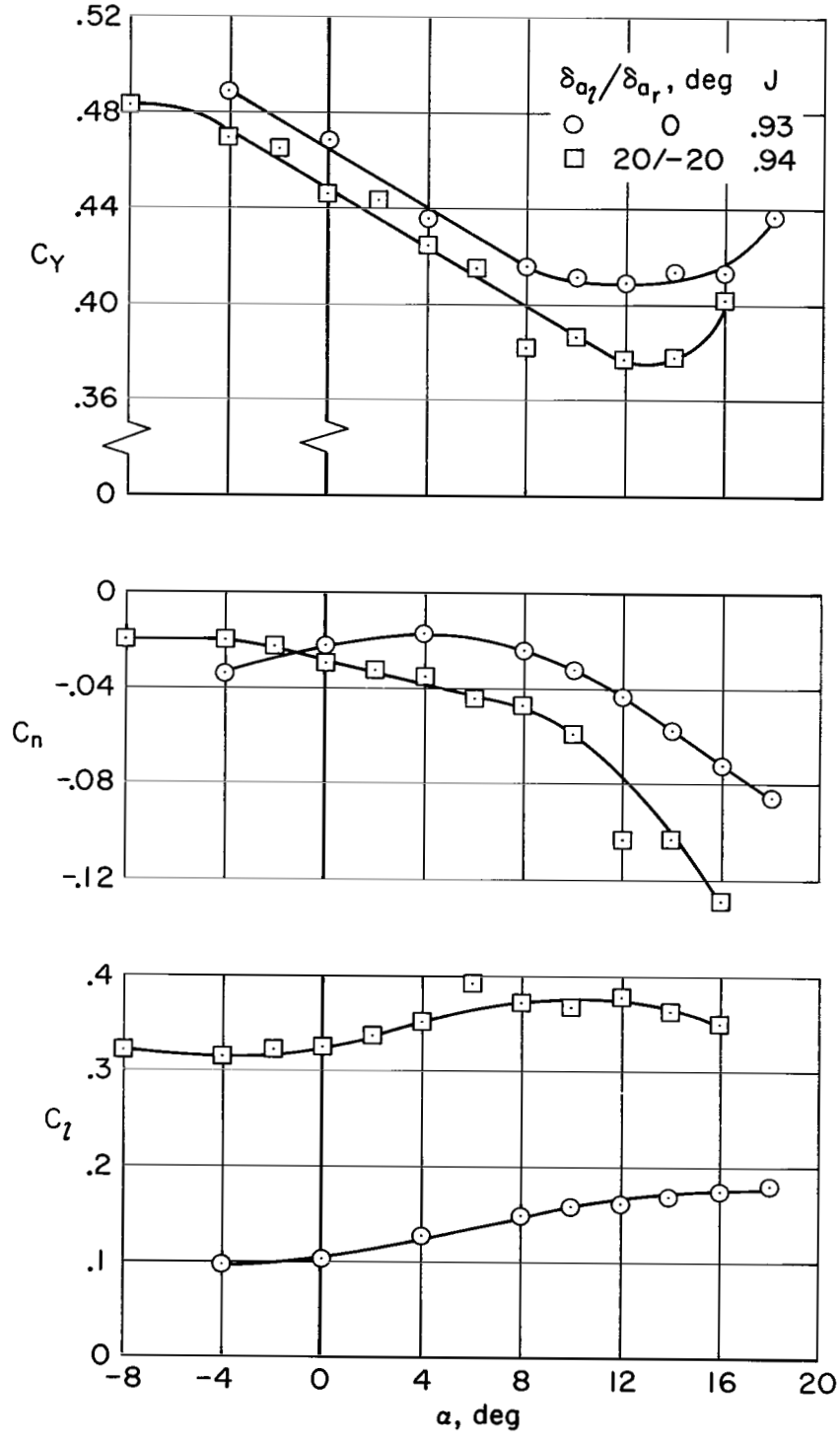

(b) $\delta_{D_f}/\delta_{D_a}$ = 5°/0°, V = 80 knots, β = -8°

Figure 15.- Continued.

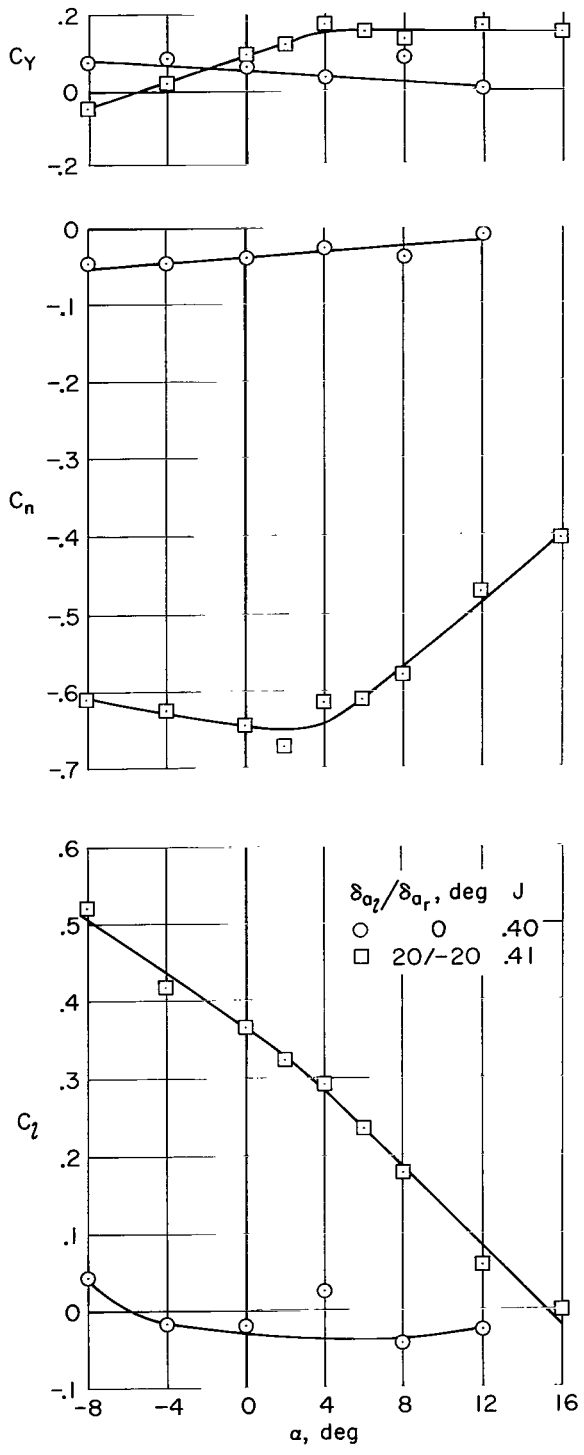

(c) $\delta_D = 50^\circ$, V = 35 knots, $\beta = 0^\circ$

Figure 15.- Continued.

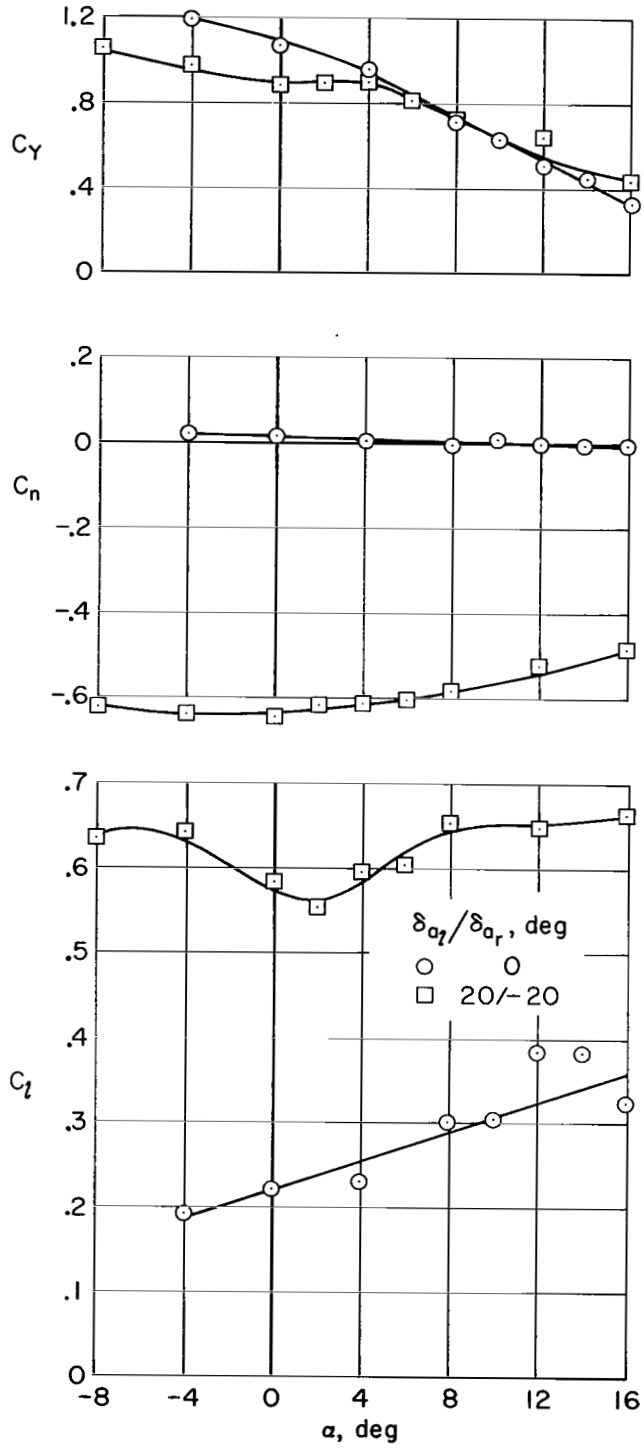

(d) $\delta_D = 50^\circ$, V = 35 knots, J = 0.41, $\beta = -8^\circ$

Figure 15.- Continued.

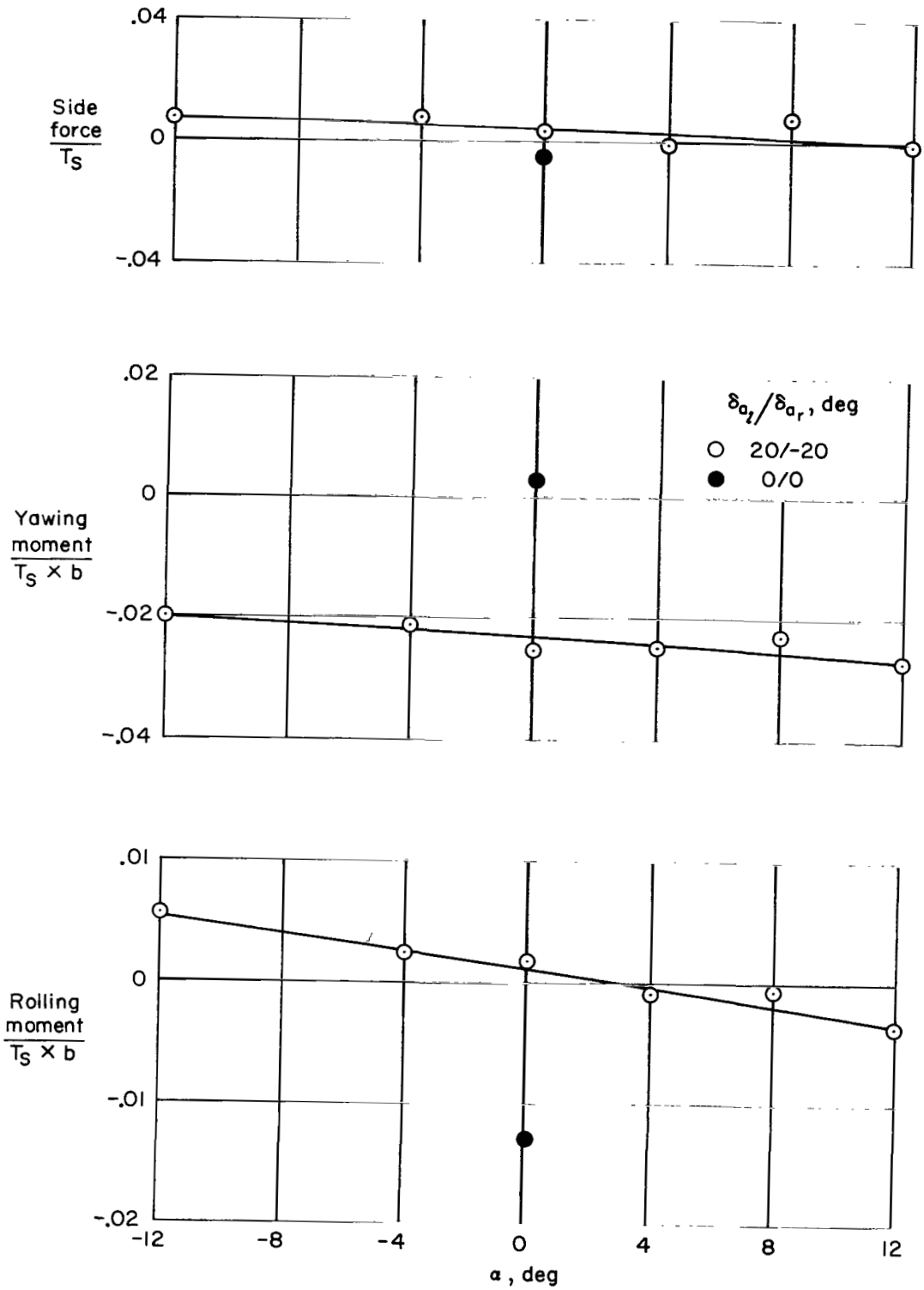

(e) $\delta_D = 80°$, V = 0, $\beta = 0°$, N = 2168 rpm, $\delta_{a_l}/\delta_{a_r} = 20°/-20°$

Figure 15.- Concluded.

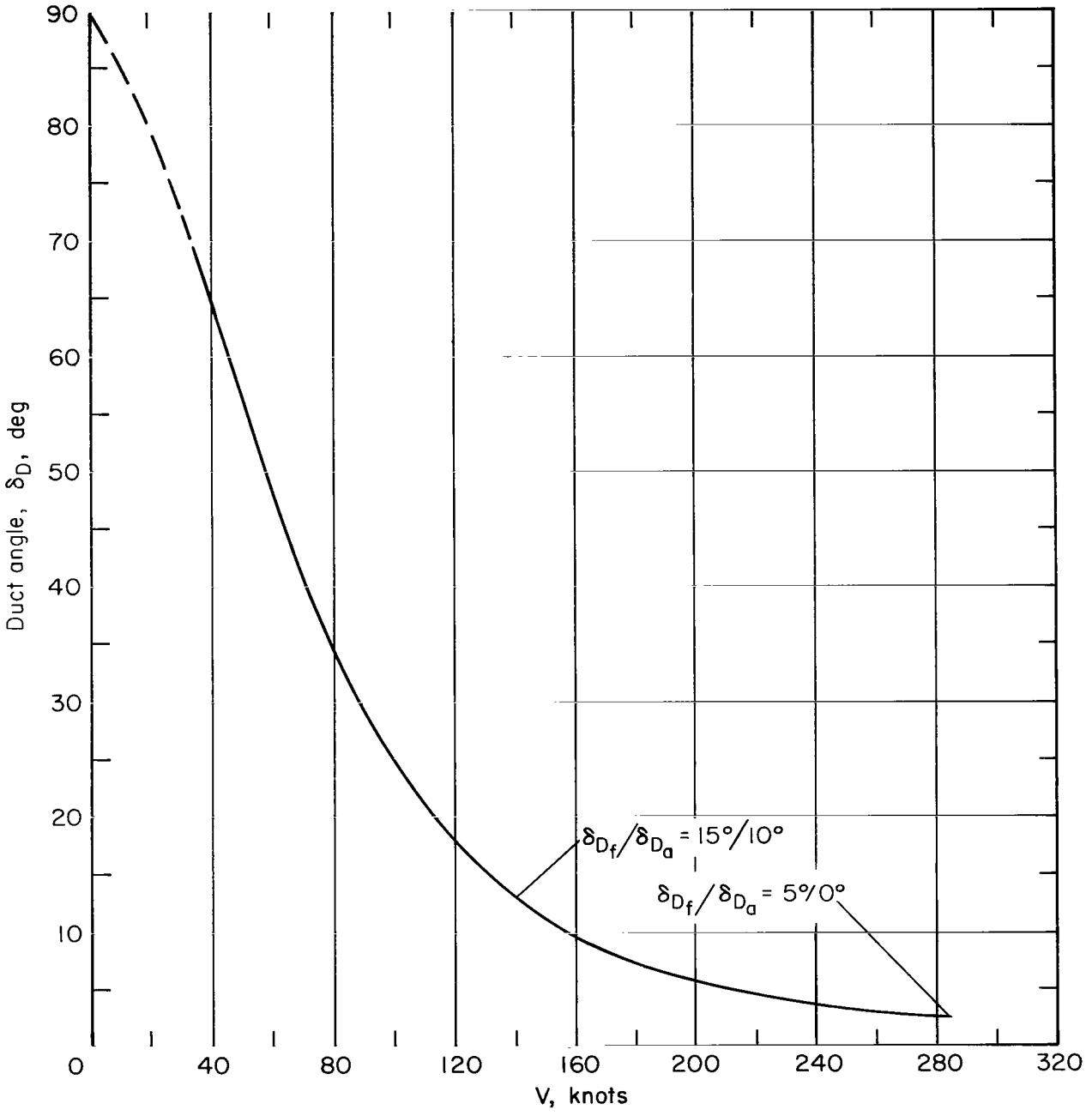

Figure 16.- Duct incidence required for transition from hover to cruising flight at level, unaccelerated flight conditions; pitching moments trimmed, lift = 6500 lb, $\alpha = 0^{\circ}$.

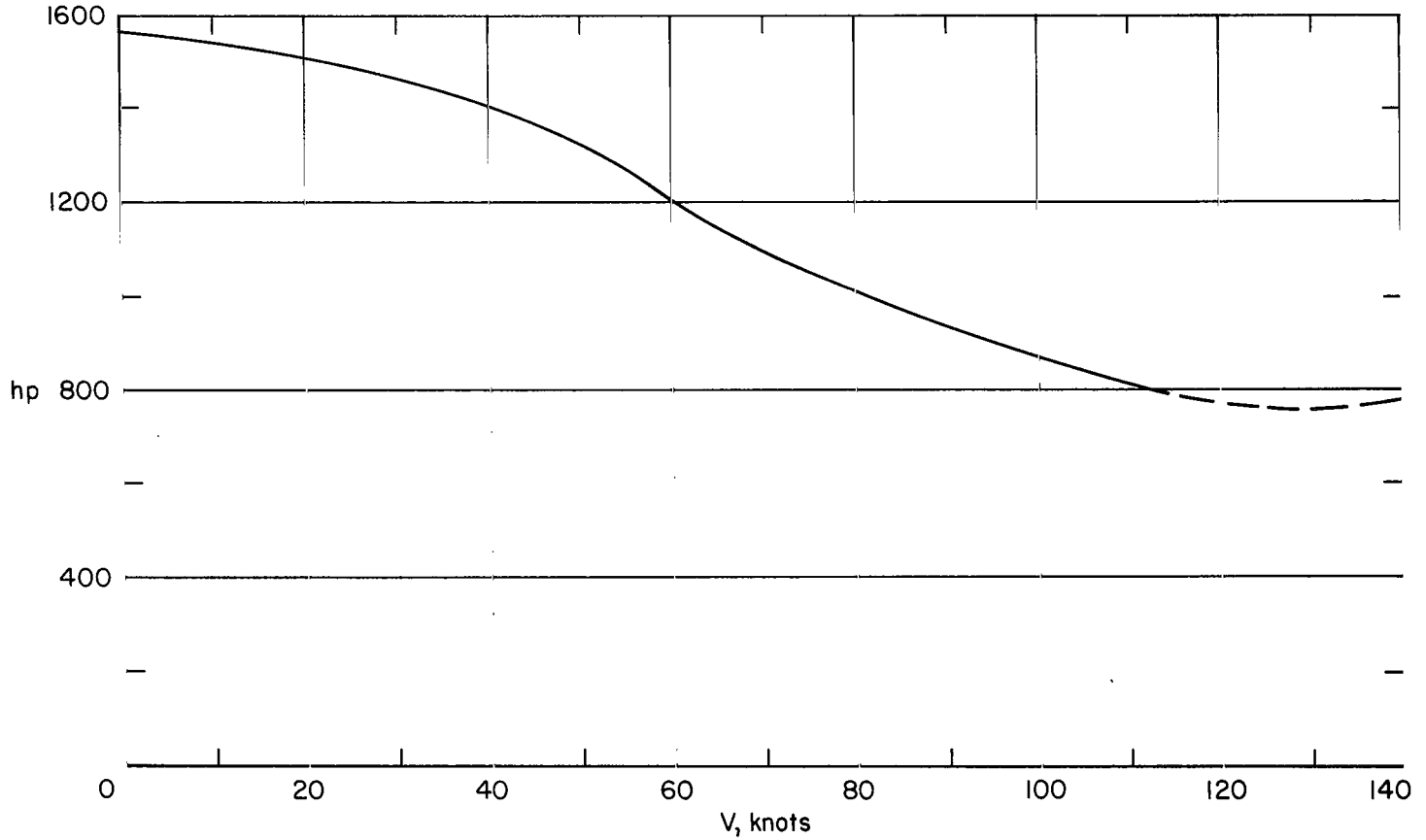

Figure 17.- Power required for transition from hover to cruising flight at level, unaccelerated flight conditions; pitching moments trimmed, lift = 6500 lb, $\alpha = 0^{\circ}$.

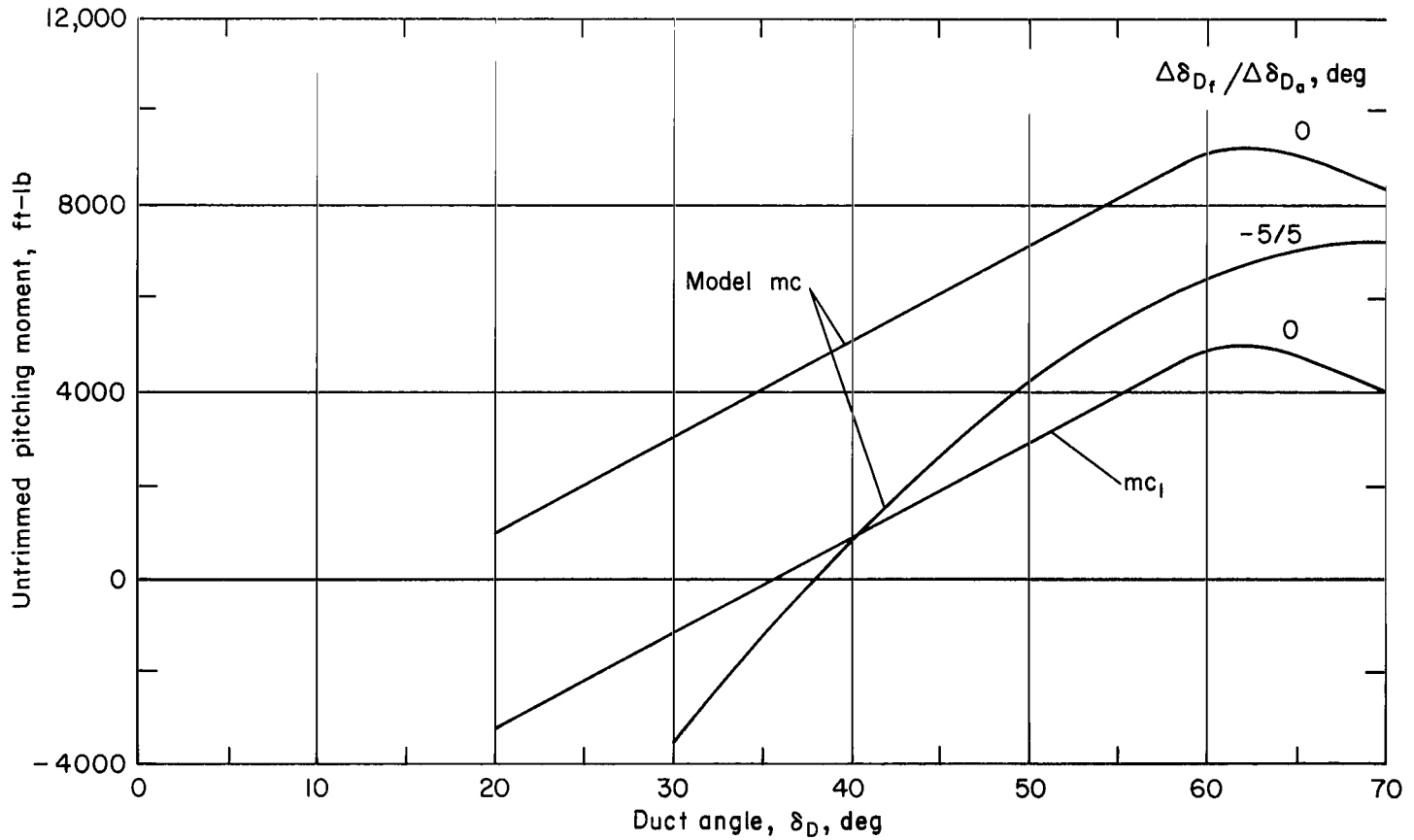

Figure 18.- Variation of pitching moment with duct incidence at level, unaccelerated transition flight conditions; lift = 6500 lb, $\alpha = 0^{\circ}$.

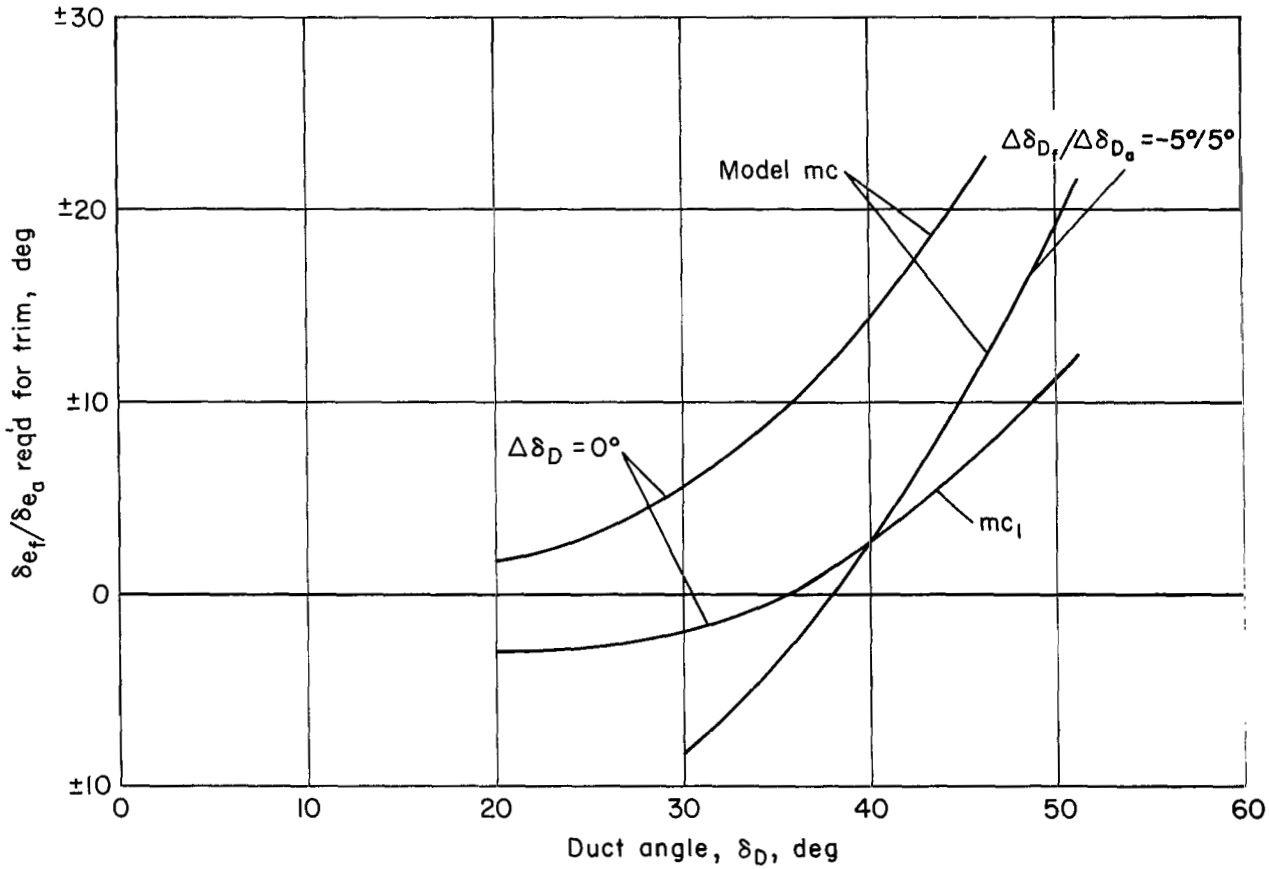

Figure 19.- Differential fore-aft duct exit vane deflection required for longitudinal trim at level, unaccelerated transition flight conditions; lift = 6500 lb, $\alpha = 0^\circ$.

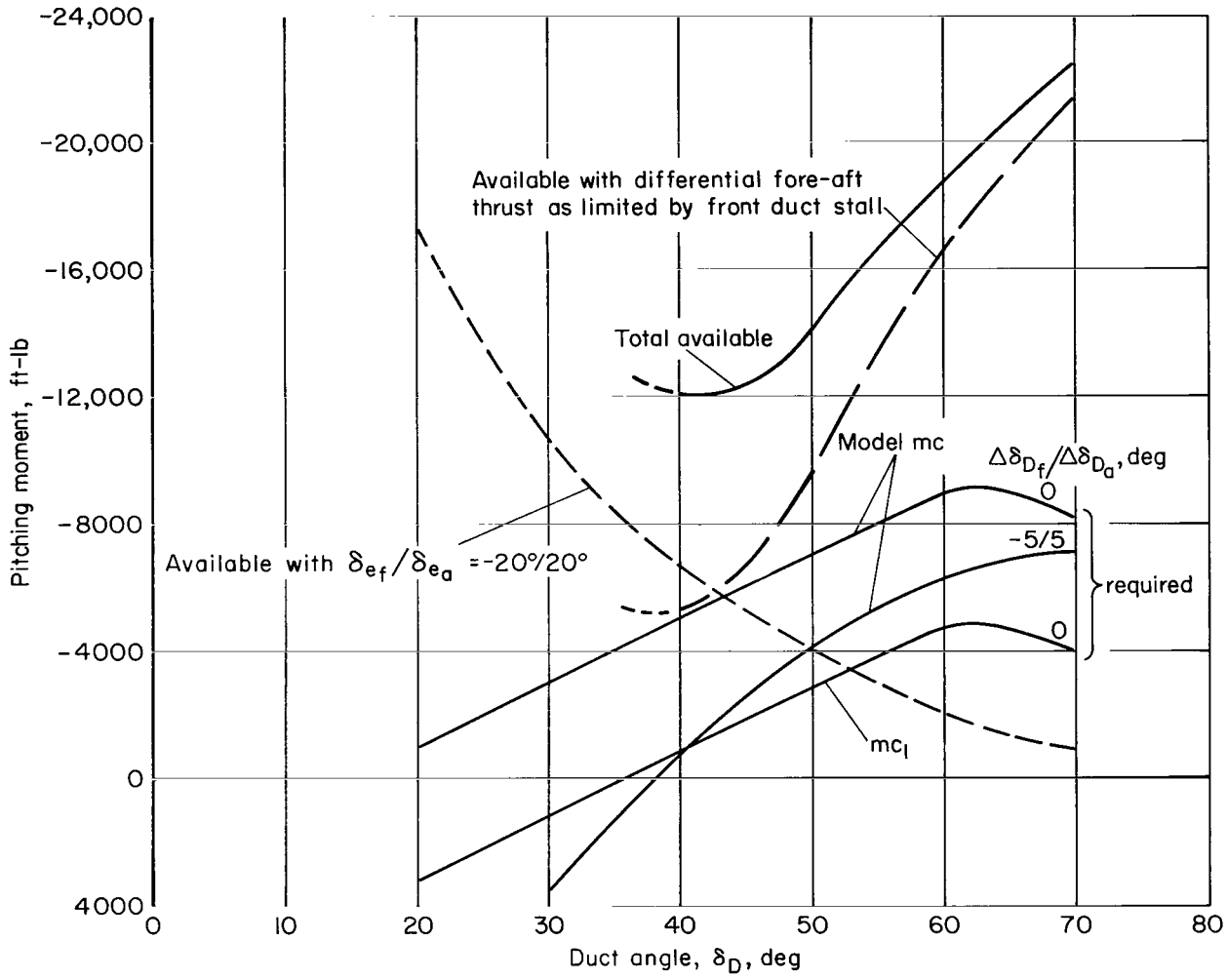

Figure 20.- Longitudinal trim requirements and available longitudinal control with differential fore-aft duct exit vane and thrust settings at level, unaccelerated transition flight conditions; lift = 6500 lb, $\alpha = 0^{\circ}$.

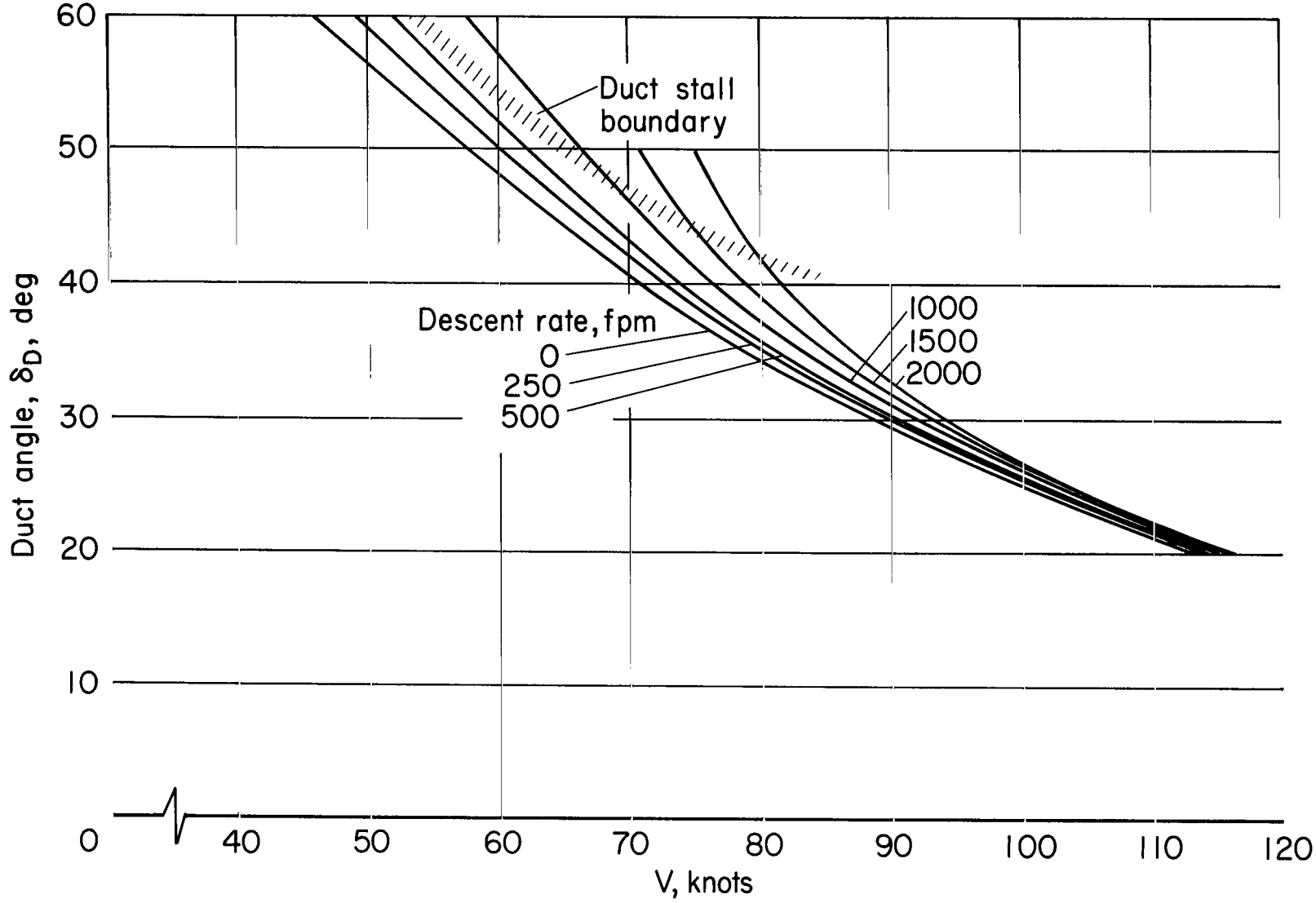

Figure 21.- Maximum descent velocities as limited by front duct stall; pitching moments trimmed, lift = 6500 lb, $\alpha = 0^{\circ}$.

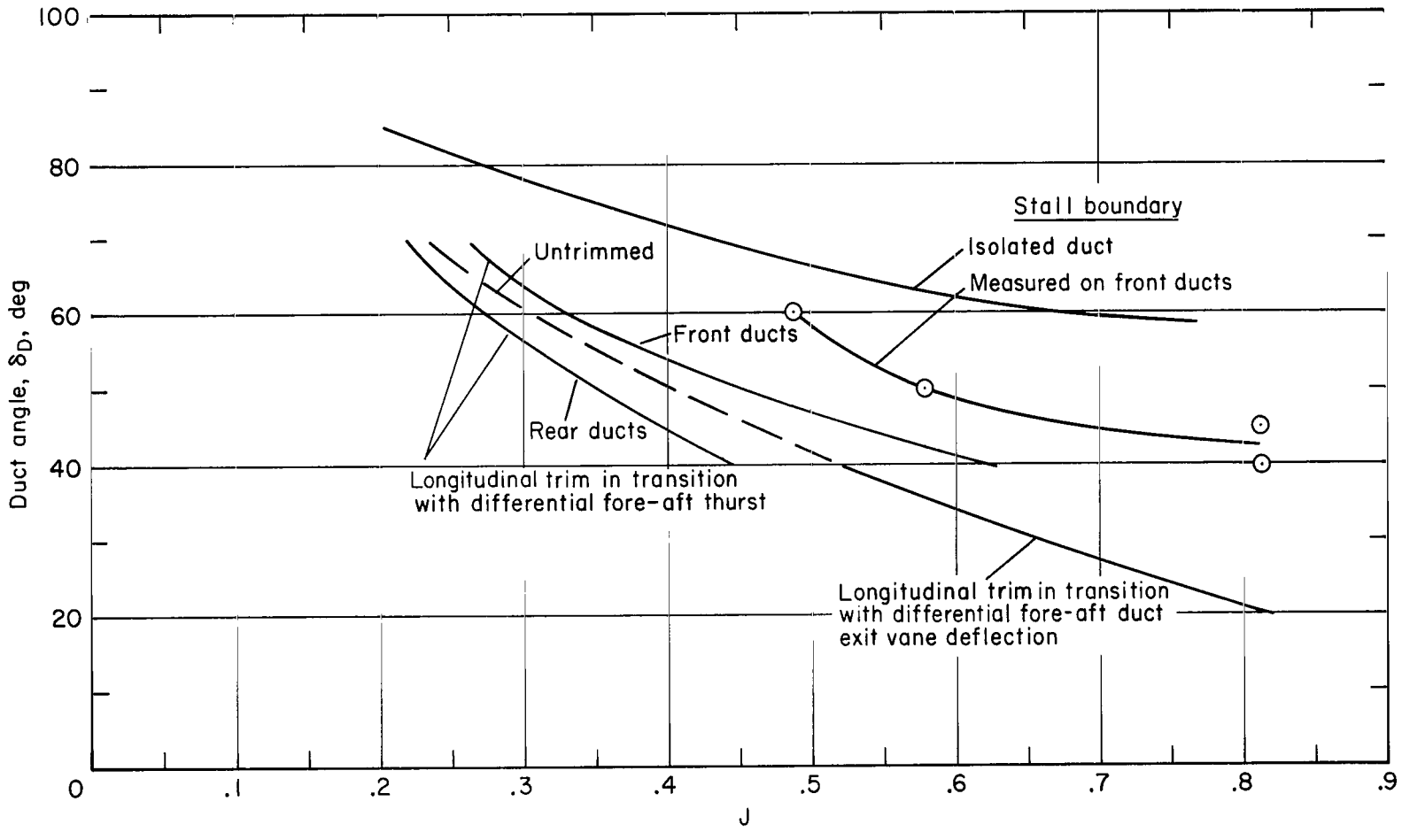

Figure 22.- Estimated duct stall margins at level, unaccelerated transition flight conditions; lift = 6500 lb, $\alpha = 0^{\circ}$.

"The aeronautical and space activities of the United States shall be conducted so as to contribute . . . to the expansion of human knowledge of phenomena in the atmosphere and space. The Administration shall provide for the widest practicable and appropriate dissemination of information concerning its activities and the results thereof."

—NATIONAL AERONAUTICS AND SPACE ACT OF 1958

NASA SCIENTIFIC AND TECHNICAL PUBLICATIONS

TECHNICAL REPORTS: Scientific and technical information considered important, complete, and a lasting contribution to existing knowledge.

TECHNICAL NOTES: Information less broad in scope but nevertheless of importance as a contribution to existing knowledge.

TECHNICAL MEMORANDUMS: Information receiving limited distribution because of preliminary data, security classification, or other reasons.

CONTRACTOR REPORTS: Technical information generated in connection with a NASA contract or grant and released under NASA auspices.

TECHNICAL TRANSLATIONS: Information published in a foreign language considered to merit NASA distribution in English.

TECHNICAL REPRINTS: Information derived from NASA activities and initially published in the form of journal articles.

SPECIAL PUBLICATIONS: Information derived from or of value to NASA activities but not necessarily reporting the results of individual NASA-programmed scientific efforts. Publications include conference proceedings, monographs, data compilations, handbooks, sourcebooks, and special bibliographies.

Details on the availability of these publications may be obtained from:

SCIENTIFIC AND TECHNICAL INFORMATION DIVISION

NATIONAL AERONAUTICS AND SPACE ADMINISTRATION

Washington, D.C. 20546